FACULTY OF INFORMATION TECHNOLOGY AND ELECTRICAL ENGINEERING

DIFFERENTLY STAINED WHOLE SLIDE IMAGE REGISTRATION TECHNIQUE WITH LANDMARK VALIDATION

Aliina Ojala

Masters' Thesis
Degree Programme in Computer Science and Engineering
June 2023

Ojala A. (2023) Differently Stained Whole Slide Image Registration Technique with Landmark Validation. University of Oulu, Faculty of Information Technology and Electrical Engineering, Degree Programme in Computer Science and Engineering. Master's Thesis, 58 p.

ABSTRACT

One of the most significant features in digital pathology is to compare and fuse successive differently stained tissue sections, also called slides, visually. Doing so, aligning different images to a common frame, ground truth, is required. Current sample scanning tools enable to create images full of informative layers of digitalized tissues, stored with a high resolution into whole slide images. However, there are a limited amount of automatic alignment tools handling large images precisely in acceptable processing time. The idea of this study is to propose a deep learning solution for histopathology image registration. The main focus is on the understanding of landmark validation and the impact of stain augmentation on differently stained histopathology images. Also, the developed registration method is compared with the state-of-the-art algorithms which utilize whole slide images in the field of digital pathology.

There are previous studies about histopathology, digital pathology, whole slide imaging and image registration, color staining, data augmentation, and deep learning that are referenced in this study. The goal is to develop a learning-based registration framework specifically for high-resolution histopathology image registration. Different whole slide tissue sample images are used with a resolution of up to 40x magnification. The images are organized into sets of consecutive, differently dyed sections, and the aim is to register the images based on only the visible tissue and ignore the background. Significant structures in the tissue are marked with landmarks.

The quality measurements include, for example, the relative target registration error, structural similarity index metric, visual evaluation, landmark-based evaluation, matching points, and image details. These results are comparable and can be used also in the future research and in development of new tools. Moreover, the results are expected to show how the theory and practice are combined in whole slide image registration challenges. DeepHistReg algorithm will be studied to better understand the development of stain color feature augmentation-based image registration tool of this study. Matlab and Aperio ImageScope are the tools to annotate and validate the image, and Python is used to develop the algorithm of this new registration tool.

As cancer is globally a serious disease regardless of age or lifestyle, it is important to find ways to develop the systems experts can use while working with patients' data. There is still a lot to improve in the field of digital pathology and this study is one step toward it.

Key words: Digital pathology, Whole slide image registration, Stain augmentation, Landmark validation, Deep learning.

Ojala A. (2023) Eri Menetelmin Värjättyjen Virtuaalinäytelasien Rekisteröintitekniikka Kiintopisteiden Validointia Hyödyntäen. Oulun yliopisto, Tieto- ja sähkötekniikan tiedekunta, Tietotekniikan maisteriohjelma. Diplomityö, 58 p.

TIIVISTELMÄ

Yksi tärkeimmistä digitaalipatologian ominaisuuksista on verrata ja fuusioida peräkkäisiä eri menetelmin värjättyjä kudosleikkeitä toisiinsa visuaalisesti. Tällöin keskenään lähes identtiset kuvat kohdistetaan samaan yhteiseen kehykseen, niin sanottuun pohjatotuuteen. Nykyiset näytteiden skannaustyökalut mahdollistavat sellaisten kuvien luonnin, jotka ovat täynnä kerroksittaista tietoa digitalisoiduista näytteistä, tallennettuna erittäin korkean resoluution virtuaalisiin näytelaseihin. Tällä hetkellä on olemassa kuitenkin vain kourallinen automaattisia työkaluja, jotka kykenevät käsittelemään näin valtavia kuvatiedostoja tarkasti hyväksytyin aikarajoin. Tämän työn tarkoituksena on syväoppimista hyväksikäyttäen löytää ratkaisu histopatologisten kuvien rekisteröintiin. Tärkeimpänä osa-alueena on ymmärtää kiintopisteiden validoinnin periaatteet sekä eri väriaineiden augmentoinnin vaikutus. Lisäksi tässä työssä kehitettyä rekisteröintialgoritmia tullaan vertailemaan muihin kirjallisuudessa esitettyihin algoritmeihin, jotka myös hyödyntävät virtuaalinäytelaseja digitaalipatologian saralla.

Kirjallisessa osiossa tullaan siteeraamaan aiempia tutkimuksia muun muassa seuraavista aihealueista: histopatologia, digitaalipatologia, virtuaalinäytelasi, kuvantaminen ja rekisteröinti, näytteen värjäys, data-augmentointi sekä syväoppiminen. Tavoitteena on kehittää oppimispohjainen rekisteröintikehys erityisesti korkearesoluutioisille digitalisoiduille histopatologisille kuville. Erilaisissa näytekuvissa tullaan käyttämään jopa 40-kertaista suurennosta. Kuvat kudoksista on järjestetty eri menetelmin värjättyihin peräkkäisiin kuvasarjoihin ja tämän työn päämääränä on rekisteröidä kuvat pohjautuen ainoastaan kudosten näkyviin osuuksiin, jättäen kuvien tausta huomioimatta. Kudosten merkittävimmät rakenteet on merkattu niin sanotuin kiintopistein.

Työn laatumittauksina käytetään arvoja, kuten kohteen suhteellinen rekisteröintivirhe (rTRE), rakenteellisen samankaltaisuuindeksin mittari (SSIM), sekä visuaalista arviointia, kiintopisteisiin pohjautuvaa arviointia, yhteensopivuuskohtia, ja kuvatiedoston yksityiskohtia. Nämä arvot ovat verrattavissa myös tulevissa tutkimuksissa ja samaisia arvoja voidaan käyttää uusia työkaluja kehiteltäessä. DeepHistReg metodi toimii pohjana tässä työssä kehitettävälle näytteen värjäyksen parantamiseen pohjautuvalle rekisteröintityökalulle. Matlab ja Aperio ImageScope ovat ohjelmistoja, joita tullaan hyödyntämään tässä työssä kuvien merkitsemiseen ja validointiin. Ohjelmointikielenä käytetään Pythonia.

Syöpä on maailmanlaajuisesti vakava sairaus, joka ei katso ikää eikä elämäntyyliä. Siksi on tärkeää löytää uusia keinoja kehittää työkaluja, joita asiantuntijat voivat hyödyntää jokapäiväisessä työssään potilastietojen käsittelyssä. Digitaalipatologian osa-alueella on vielä paljon innovoitavaa ja tämä työ on yksi askel eteenpäin taistelussa syöpäsairauksia vastaan.

Avainsanat: Digitaalipatologia, Virtuaalinäytelasien rekisteröinti, Värien augmentointi, Kiintopistevalidointi, Syväoppiminen.

TABLE OF CONTENTS

FOREWORD

Working with a topic of digital pathology has given me new insights of utilizing computer engineering in an important field of science. During the journey of medical literature and computer engineering studies I have been involved in fascinating world of research, and I believe this experience to open interesting new doors for my future career. It has been a nice challenging task to dive into the topic of digital pathology.

The purpose of this work is to find new ways to develop an algorithm that helps in registering whole slide images by using landmark validation. Those images are scanned from the tissues that may have cancer cells in them. By investigating those samples, pathologists can more easily find some microscopic but extremely significant cell changes, and hence be able to analyze and provide a correct treatment for the patients suffering from cancer. The tool to be developed in this work is about detection of tissue slides by using landmark validation, the little marks that usually pathologists have added on the samples. Saying it more beautifully, this topic can save lives.

My brilliant supervisor Dr. Anja Keskinarkaus has advised me by providing her vast knowledge, earlier research papers, suitable limits for this work, and clear instructions how to proceed in this new situation. Then, my great second supervisor and technical advisor Md. Ziaul Hoque has helped me with the coding parts by giving me lot of examples and many tools to compare the registered image data to the source image, and with his constant support whenever needed. Both of them have helped me to get into this topic and made me feel welcome in this project during our monthly live and remote meetings. I also want to thank Pia Nyberg for the possibility to visit Biobank Borealis of Northern Finland. Many thanks to my fiancée and our families being so great helpers as they have supported me and my ideas during this journey. Also, special thanks to my mum who tried to read the thesis almost in the end of the process, but after seeing the number of pages she decided to save the reading experience for the future. I want to thank you all for your time, nice supportive words and traveling company within the months of the writing process.

This work has been written during the academic year 2022-2023 in Oulu, Tampere, Helsinki, Tallinn, Paris, London airspace, and finally finished in Kiikoinen.

Kiikoinen, June 19, 2023

Aliina Ojala

LIST OF ABBREVIATIONS AND SYMBOLS

A	1st registration transformation parameter
$\bar{A}$	Respective estimator of A
C	Curvature
$c_{1,2}$	Variable to stabilize the division with weak denominator
$D_{i,j}$	Stain density map
$G_{1,2}$	Gradient map of the image
H	Image height
I_{ij}^{*}	Augmented image
I_o	Illuminating light intensity
I_{RGB}	Whole slide image
L	Warped subject image patch
$M_{i,j}$	Stain color matrix
N	Negative Normalized Cross-correlation
$PC_{1,2}(x)$	Phase congruence
$PC_m(x)$	Phase congruency measure
R	Target image patch
r	Scaling factor
S_1	Luminance
S_2	Contrast
s	2nd registration transformation parameter
$\bar{s}$	Respective estimator of s
${s_x}^2$	Local variance of x
${s_y}^2$	Local variance of y
$s_{x,y}$	Local covariance between x and y
$S_G(x)$	Similarity measure of gradient magnitude
$S_L(x)$	Similarity score
$S_{PC}(x)$	Similarity measure for phase congruency
$T_{1,2}$	Positive constant
v	Displacement field
W	Image width
x	Reference image
$\bar{x}$	Local mean of x
y	Registered image
$\bar{y}$	Local mean of y
α_i	Interpolation coefficient
α_n	Regularisation parameter
Ω	Whole spatial domain

λ	Uniform distribution parameter in range [0,1]
μ_x	Respective mean of reference image
μ_y	Respective mean of registered image
σ	Scalar feature of 1 pixel
2D	Two-dimensional
3D	Three-dimensional
AI	Artificial Intelligence
ANHIR	Automatic Non-rigid Histological Image Registration
CLAHE	Contrast Limited Adaptive Histogram Equalization
CNN	Convolutional Neural Network
COAD	Colon Adenocarcinoma
CT	Computed Tomography
DL	Deep Learning
FSIM	Feature Similarity Index Metric
GPU	Graphics Processing Unit
H&E	Hematoxylin and eosin
ML	Machine Learning
MRI	Magnetic Resonance Imaging
ORB	Orientated FAST and Robust BRIEF
PCC	Pearson Correlation Coefficient
PET	Positron Emission Tomography
RGB	Red-green-blue
RMSE	Root Mean Square Error
SIFT	Scale-Invariant Feature Transform
SSIM	Structural Similarity Index Metric
SURF	Speeded-Up Robust Feature
rTRE	Relative Target Registration Error
TME	Tumor Microenvironment
TRE	Target Registration Error
WSI	Whole Slide Images

1 INTRODUCTION

Cancer is globally a major life-threatening problem in health, and it is defined as a tissue mass consisting of genetically modified cells which cannot respond correctly to normal mechanisms of cellular growth [1, 2]. The new digital methodologies and technologies provide more effective ways in cost and time to obtain the digital images in digital pathology. With the virtual biological tissue samples the patients can be given the correct cancer diagnosis quicker without compromising the diagnosis quality [3] compared to the traditional ways of histopathology. That is why biomedical imaging is used as one of the most crucial data modalities in a world of cancer research [1].

Whole slide imaging (or whole slide image), also known as WSI, has now been developed the last two decades to be a universal digital imaging tool in histopathology by allowing entire tissue sample slides to be imaged and stored stably with a high resolution [4]. In the process of digital pathology developing, the histological slides are scanned by using the advanced micro-scanners and then stored permanently as WSIs [5]. The images produced by WSI scanners are full of significant information of the layers of digitalized samples. Images' complexity is way higher compared to the many other imaging methods due to their large size and high resolution (common resolution may be even 100k × 100k pixels), presence of color information (usually hematoxylin and eosin stains) and the availability of multiple scales of information (such as scales 4×, 20×, and 40×), for example. In the light of these numbers, it is clear, that a human reader is not able to extract all of this visual information as easily as the digital systems [4].

There are several ways to utilize digital pathology and tools to help the daily work of pathologists. As the world is digitalized in many ways nowadays, the possibility of digital stain samples opens doors for global markets and research in the area of histopathology. The digital samples in cloud databases enable people around the world to be involved in the research of the cancerous cells. Ciompi et al. say in their study [6] that the decision whether a patient should be treated with adjuvant chemotherapy mostly depends on the stage of tumor, and the patients diagnosed with the same stage of disease may still have considerable varied findings. This has led to the investigations of histological parameters as new biomarkers to guide pathologies for more accurate decisions of adjuvant treatment. The downside of using biomarkers is their manual assessment that currently suffers from high inter- and intra-observer variability and limited clinical applicability. Whole slide histopathology images could extend the enhancement of these reproducible imaging biomarkers.

1.1 Thesis Objectives and Targets

The main idea of this study is to develop a stain color feature augmentation -based image registration tool to help the research work in the future. The purpose is to compare the developed registration algorithm with the state-of-the-art algorithms that are registering

the stained histopathological tissue samples from whole slide images. An interesting part of the outcomes is to measure the Pearson Correlation Coefficient (PCC), Structural Similarity Index Metric (SSIM), Feature Similarity Index Metric (FSIM), Root Mean Square Error (RMSE), relative Target Registration Error (rTRE), robustness, and the other image details. The same metrics are measured in previous studies so comparison between different registration techniques is possible. This thesis work has an overview about literature of important sights of digital pathology in cancer research and the purpose is to develop a stain color feature augmentation tool utilizing landmark validation. In the end of this study there are results showing how the theory and practice are combined in our proposed model. The previous research and literatures indicate that there are various ways to improve the staining methods and develop the stain augmentation and registration techniques. There are topics of digital pathology, tissue staining, color normalization, data augmentation, imaging, and registration referenced in later chapters of this study. The focus is on stain color feature augmentation phase in registration process within the knowledge of previous research. Using a registration technique of stained WSIs as a cancer detection tool is a significant way to observe cancer cells in microscopic imaging scale.

Public dataset from Automatic Non-rigid Histological Image Registration (ANHIR) challenge are observed during the work but also myoma tissues are studied. Collection of the myoma samples is approved by the ethical committee of the Northern Ostrobothnia Hospital District. The datasets differ from each other in size, publisher (public versus private availability indicates the earlier use of the datasets), magnification, stain, and data as ANHIR set consists of many kinds of tissues with landmarks but myoma set includes only non-landmarked myoma tissues.

Artificial Intelligence (AI) already gives pathologists a possibility to identify unique imaging markers to improve early detection, determine prognosis, and select the suitable treatments in disease processes. That means, that pathologists are able to serve more patients fighting against cancer while diagnostics are well maintained, and accuracy is prognosed [4]. With this topic I am giving a view over the methods that can be used during the image registration phase. I also believe that this kind of work will help the cancer patients in the future and it makes this study process feel even more valuable. The topic is globally significant, and the subject of developing the tools helping people with serious illness should be studied more. By measuring the quality of the registration methods, it is possible to find an important aspect to understand the different potential algorithms and their functions. Comparing the models can also provide notable evaluation values for registration process and hence give a great advantage in the future studies.

1.2 Digital Pathology

Histological samples enable experts to see the different layers of the sample tissues and various types of cells' forming. The tissues are studied under the microscope and it allows seeing the microscopic composition of samples that a bare human eye could not see. Usually, the normal microscopic structures of the tissue are studied and thus the possible changes are noticed during any disease process. Generally, the term of digital pathology refers to the composition of digital workflow and imaging solutions. These solutions are appointed toward building a digital image-based practice environment where WSIs and other digital images are obtained, searched, managed, and interpreted for specific content [7]. The diagnosis is called histopathology when the tissue or cell is affected by a disease. A tissue is cut from a patient for a detailed inspection and histologist prepares it to find out the damaged cell or tissue caused by an abnormality, a possible disease [8]. Pathology itself is the field of study where the disease process is under an interest, and it includes examining the physical and histological changes of tissues. It means, that the diseases caused by changes in a particular organ, tissue, or cells are studied. Janowczyk et al. [9] describe digital pathology to be a process that enables histology slides to be digitized to produce high-resolution images by using WSI scanners. It is essential to understand all possible variances in morphology, texture, and color appearances when developing an algorithm for a nuclei segmentation, as an example. Deep learning (DL) can be used as a great tool for feature learning as it can iteratively improve the learned events of the given data. The process of digital pathology has a determining role in modern clinical practice and it is progressively demanded as a technological requirement in the scientific laboratory environment. Especially the advantages of digitalization, such as faster networks and cheaper and bigger storage solutions, have helped experts to manage digital slide images, and share them around the world for clinical use [4]. Digital pathology image analysis suits ideally for the events that could be missed while using conventional microscopy, for example by screening whole brain tissues such as microhemorrhages [10].

In regions where patient populations are scattered over wide geographical areas, such the Scandinavia region and Canada, the use of digital pathology is remarkably common. Even though the expertise may be located only in the largest center areas, experts can share their materials and findings digitally by utilizing the digital pathology tools [11]. Digital pathology provides very fascinating and highly dense data, but at the same time it has an interesting future challenge in the field of multimodal data fusion; making therapy diagnosis and recommendations, also called as theragnosis. It would be exciting to have this kind of solution as it concerns personalized medicine. Already a decade ago, it was written that we are living an eventful time where disease diagnostics and treatment are becoming more accurate and patient specific. Digitalization is an increasing trend and computerized imaging methods are assisting the experts of pathology and radiology in

making precise diagnosis of diseases. With those digitalized images it is also possible to identify morphological features correlated with prognosis and hence find the accurate treatment paths. Also, molecular profiling of disease should suggest new more effective therapeutics and help the clinician understand the underlying biology of the disease even better [12]. For example, in a field of oncology and precision medicine there is a great potential in digital pathology and AI. The digital workflow innovation could change the way the cancer diagnoses occur, with the benefits of shared data and images, collaboration possibilities through multidisciplinary conferences, more efficient and integrated diagnostics, improvements of patient care and safety, improved accountability, and cost and time savings by optimizing staff performance. With the help of AI many manual tasks can become automated and more standardized [4].

1.3 Imaging and Registration

Digital pathology is also called as virtual microscopy or whole slide imaging because it is the conversion of the light microscope image, a slide of a set of digitized files. Digitization allows image manipulation and can derive its hidden information of diagnostics. Image registration is a regular task in many medical and biomedical image analysis applications [13, 14]. Computer science has many advantages in the field of medical imaging, it has led to the methods for image processing which usually allow visualizing objects inside the human body. Those methods are useful especially in medical research, diagnosis, and treatment planning. In most cases, the integration of useful data gained from separate images is the key what comes to the clinical diagnosis. Thus, for better observation, the images should be geometrically aligned. Image registration is a procedure where the reference image's mapping points are corresponding to another image's points. The process is about determining the correspondence of features between the images taken at numerous times or using various imaging modalities. Registration is mostly used to correct the different patient positions between the scans. The reference and the referred images may vary as those images have possibly been taken many times by using different techniques and several angles to get two-dimensional (2D) and three-dimensional (3D) perspectives [15, 16].

Structural devices like computed tomography (CT) and ultrasound, plus functional devices such as positron emission tomography (PET), magnetic resonance imaging (MRI), and single photon emission computed tomography are the most common imaging techniques. Also, the correspondences are sometimes used to change the appearance by rotating, translating, or even stretching the images. Registered imaging scan parameters that affect the sampling integrity and the size of the resolution are called voxels [15-17]. Two decades ago, typical structural state-of-the-art MRIs of human brains had voxel sizes of $2 \times 2 \times 2$ mm^3, and a decade ago voxel sizes were already smaller than $1 \times 1 \times 1$ mm^3 [18, 19]. The registration in clinics is generally performed based on the 3D reconstruction

of scanned 2D thin slices, building a high-resolution pathological image [20]. Integration of pathology image analysis and radiomics is an important combination as routine radiology imaging modalities like CT, PET, and MRI, are high in value for cancer screening and monitoring. In radiology, cancer imaging is noninvasive compared with pathology, and it can often capture also physiological and pathological features in organ- and system-level [21].

1.4 Whole Slide Image Registration

Already for many decades, pathologists have been diagnosing patients with help of digital images of glass microscope [11]. Whole slide imaging is a result of modern technology where glass slides are scanned to generate digital images. These whole slide images can be handled as digital files, and most of the WSI viewers support measuring areas and lengths so the digital slides can be used for viewing images, storing annotations, and measuring them [22, 23]. Whole slide images of tissue samples contain a huge amount of information that is mostly unseen by a human eye. This information was previously available only for a well-trained pathologist or biotechnologist who had an experience in a field. Quantifying the biomarkers, image analyzing can bring a valuable advantage to standardize the analysis as well as minimize bias and variability in the generated data [10]. It is very important to have accurate diagnosis and prognosis while selecting and planning the treatment for cancer patient. WSI is now becoming a routine in medical environment and clinical procedure with its rapid advantages [21]. Images that are rich in information may still be difficult to process entirely from a computational point of view, and some less informative regions can exist in the images [10].

Using high-quality WSI scanners enables pathologists and researches to deliver a large amount of image data and show extensive context and microscopic details both at the same time. The scanners are capable of quickly and effectively digitizing histological tissue sample slides without any considerable manual effort. These scanners can generate vast amounts of digitalized data in high resolution since a single image can be even several gigapixels in resolution [24]. Some WSI scanners can scan at multiple focus layers, but the time of scanning increases linearly with the number of layers. By stacking the layered images all together they can provide a 3D image stack. The great advantage of digital image viewers is a possibility to display several slides side by side so the structural details of each slide and different stains of the same tissue area are easier to measure and compare [22]. WSI is increasingly used in research applications, consultation, and external quality assurance practices. In the best case it can also offer improvements in the safety, quality, and efficiency of a histopathology department [11].

The digital scanning technology and the increasing availability of large datasets together have given pathologists a possibility to co-operate with technology experts, data scientists, engineers, and imaging physicists to investigate a new potential tool for

pathology. That tool is machine vision, a modern component of computational image analysis. One of its biggest advantages in the field of pathology is to extract and generate quantitative data from subject matter of digital images [7]. WSI technology is already widely used for presentations, teaching at conferences, virtual workshops, and of course in tumor boards. AI tools equipped with WSI can help notably the next generation of pathologists in their training process, as it can provide standardized and interactive digital tissue slides that can be shared at any time with multiple users anywhere. This kind of interactive tool enables trainees to view and zoom the digital slides at the same time, and hence provides the real-time tutorials in a dynamic environment [4, 25].

1.4.1 Applications of Image Registration

A modern workflow of pathology is digitalized so that the scanned histology slides can be viewed on computer screens. Digitalization enables pathologists to identify and measure the same events on tissue sections digitally that earlier were observed on a microscope [10]. It is said [26] that the term of image analysis has been created already in the 17th century when the microscopic objects' measuring system was developed, so the origin of image analysis with objective tools seems to be as old as an idea of microscope itself. The term describes the meaningful information pathologist get from images in an objective and reproducible way. Digital slide scanners have been commercially available from the year 2000 and from that time also WSI has become increasingly more common [10].

Image registration is a process where the geometric transformation unites identical anatomic points in two image series of a moving and a static source datasets. In image fusion the mapped data is combined from the moving dataset with the static one. The function that is applied to the moving image to align to the static image is called as a transformation. Rigid registration describes the transformation that preserves the image's distance between its all points, and it usually includes translation and rotations in all directions [17]. Image registration has various potential applications in clinical diagnosis such as diseases of tissue, liver, and cardiac, and it is a vital tool in medical imaging. The process is about aligning two or more images into a common coordinate system to monitor the microscopic changes between the slides. Registration algorithms set correspondence between those two or more images by computing transformations [15].

Digitalization enables viewing the pathological images zoomed up to magnification of 40× on a computer screen. Zooming in the very fine details, measuring coverages and distances, and annotate the images are huge advantages in the field of histopathology [22]. In addition to view the digitalized histology slide on a computer screen, it can also be handheld device at a similar resolution as light microscopy [10], and it helps to contribute the slides in between the organizations and tutoring meetings, for example.

Medha et al. [15] have listed applications of image registration from many different fields. The list is long and contains, for instance, super-resolution image, change detection, monitoring a tumor growth, and treatment verification that are all important operations in area of digital pathology. The rest of the list consists of remote sensing, environmental monitoring, weather forecasting, map updating in cartography, integrating information into geographic information systems, and computer vision such as target localization and automatic quality control. Digitalized images can serve insights into tumor microenvironment (TME), where one essential step of TME's quantitative characterization is to segment various types of sample substructures and cells from those images. Such segmentation provides the basis for many different image analysis tasks, as cell composition, spatial organization, and substructure-specific morphological properties, to name a few [21]. To get more advantages out of digitalization in histopathology, it is notable that even more information is available with the help of AI.

1.4.2 Challenges in Whole Slide Image Registration

Histopathology images play a big role in diagnosing the cancerous diseases. The inspection of tissue samples created by WSI scanners supports pathologists to make decisions while analyzing the images, but there are also problems arising in this decision process. Borovec et al. [27] have listed the following challenges in non-rigid registration of differently stained histology images: need of fully automatic registration, extremely massive size of images, real-time requirements in clinical situations, differences in the tissue appearance causing the problem of missing data, and the last but not least, the lack of unique features due to a repetitive texture [28]. Also, the data storage costs are one of the limitations in digital pathology environments as a WSI file size can be anywhere in between few megabytes to several gigabytes. Digital archiving is one kind of solution for permanent slide storage with constant quality and lower cost [22].

Barisoni et al. [7] have listed some more disadvantages of digital pathology. For example, the limitations include the need of massive network bandwidth to manage large image sizes, and the lack of Z-dimensional focus. With these limitations many pathologists have found that sometimes digital pathology can be even more time consuming and less accurate than glass slide microscopy, that has been more traditionally used for diagnosis in a field of pathology. Whole slide image registration is challenging also due to its pyramidal structures and many levels of resolutions, unwanted artifacts, missing sections of sample preparation, and the differences in local structure between slices from the same sample [27], as well as the color variations created by sectioning, staining, mounting, and scanning processes. The pyramidal structure is demanding to handle as it requires a huge amount of memory and display characteristics on computers. Usually, it is not even possible to process WSIs on a processor with a single core [3, 29, 30].

One known problem in WSI scanners is their ability of producing digital images without a focus area when the autofocus system selects any focus point that locates in a different plane than the real height of the tissue. A simplified solution, suggested in a study of an automated blur detection [31], would be to increase the focus points by adding several extra points, but downside of this kind of solution is its slowness. That solution would probably cause long delays when scanning the slides with these extras. In our visit in Biobank Borealis of Northern Finland[1] it was shown that adding more focus points by hand the samples are more readable, but it also increases the scanning time, depending on the number of points. However, the extra points make the virtualized slides more useful as they are focused on the right structures on tissues at once. What comes to manual work, seems like AI could give an answer for it. Artificial intelligence provides a great alternative by automatically identifying out-of-focus regions and making WSI scanners chance to add these extra focal points to those unfocused regions [4]. AI, and especially DL, has recently shown a huge potential in image analysis tasks such as tumor region identification and prediction, TME characterization, and metastasis detection [21].

Tissue sample slides in histopathology are commonly prepared using special stains to examine the samples under a microscope and determine tissues that are affected by a disease. The transparent tissue samples are colored by pathologists or bioanalysts and various stains highlight particular cells and tissue structures. Those chemical stains also result in diverse occurrences on nearby tissue areas. The most common routine stains used in pathological practice are hematoxylin and eosin (H&E), where hematoxylin stain attaches with acid structures in purple and eosin dye stains eosinophilic structures in pink hues [2, 3, 32]. Color variations in digital images are mostly produced by the use of various types of WSI scanners and equipment, different staining protocols, variations in thickness of tissue samples and slides, mismatch between scanning characteristics, and several manufacturers. One way to reduce the color variation is to convert red-green-blue (RGB) image into the grayscale, but it is worth of mention that some information will be lost during that process [4, 8].

[1] https://oys.fi/biopankki/

2 BACKGROUND

Using multiple dyes during histological sample preparation may reveal distinct properties in tissue [28]. Serial section histology is commonly used when evaluating the surgical margins with multiple consecutive sections [33]. Handschuh et al. have summarized manual reconstruction of serial physical sections being the oldest known method to present micro-anatomical data in 3D format, already from the 90th century [34]. Each stain has a different slide preparation and the tissue undergoes complicated deformations. Also, due to serial sectioning, the texture of the image details may remain very similar, and all that make the process a challenging task [14, 28].

The H&E stain combination is widely used in the industry because it is relatively easy to execute. There are also other popular histological stains with different properties used by pathologists, especially to highlight better the different tissue constituents. These non-H&E stains are also known as special stains and they are mostly used as a pathologic evaluation standard in the certain disease entities, including nonneoplastic kidney, liver, and lung diseases [35]. Pathologists and experts normally monitor multiple slides and after observing they combine the visual information to form a diagnosis [30].

The development of reliable imaging biomarkers requires an accurate and reproducible classification of the main tissue components [6]. Computational pathology has a target in developing machine learning based tools to automate and streamline the analysis of WSIs. The sections are composed of small and thin tissue slices stained with different dyes to get the tissue architecture more visible under a microscope [36]. It has been noticed that the accuracy of the registration of serial sections is depending on the distance between the sections themselves and on the quality of the tissue sectioning [37]. The use of different chemicals to dye the slides determines how visible the observed structures are. Even if the tissue was dyed in proper process, there may still be some parts missing the dye and hence be unnoticeable. Also, the prices of dyes are expensive and not every dye can be used for every tissue, so it may limit the resources available.

2.1 Automatic Non-rigid Histological Image Registration Challenge

The importance and the difficulty of the histology registration were the main motivators to organize an open challenge called Automatic Non-rigid Histological Image Registration, co-organized with the IEEE ISBI 2019 conference [20, 27, 28]. The organizers provided an open dataset containing different tissue types obtained using multiple dyes, and provided an automatic and independent, server-side evaluation tool with it. The images from dataset were paired together and the landmarks for calculating Target Registration Error (TRE) were marked by histological experts. It is said that ANHIR enables information to fuse from the same tissue structures that may not be revealed by one of the applied dyes [38]. The dataset of ANHIR challenge was evaluated

in a study of hybrid deep feature-based deformable image registration [20], where it is reported that deformable image registration is a necessary technique for fusing multi-modal pathological slices and decision-making.

On the website of ANHIR challenge[2] they say that the challenge aims at the automatic non-linear image registration of 2D microscopy images of histopathology tissue samples stained with different dyes. Image alignment enables the experts to evaluate the histology for a patient in a certain area that contains multiple markers. There may be sections that have stretched or changed shape from section to section due to non-linear deformations from the former processing phases. Only a few automatic alignment tools can handle huge histological images with a proper accuracy and computational time, and this challenge was about to find the ways to improve these tools and create new ones. The registration performance is evaluated with relative Target Registration Error (rTRE). That value represents the geometric accuracy between the target and warped landmarks in the frame of target image, and the accuracy is evaluated utilizing the landmarks that are manually annotated [39].

2.2 Rigid and Non-rigid Registration

Image registration has historically been classified being rigid when the images are assumed to be rotated, translated, scaled, and sheared objects to achieve correspondence. One example of the possible rigid registration applications is to capture patient's global motion. On the contrary, in non-rigid image registration the correspondence between structures in two or more images cannot be achieved if the images are not locally stretched [16, 40]. Non-rigid registration is used in 3D modeling to fill in the scanned parts that are otherwise missed [41]. In machine vision it has been used for object and handwriting recognition [42], and with non-rigid registration it is also possible to transfer metadata from one image to another one using nearest-neighbor based techniques, meaning rendering a subject or an object with a texture taken from a whole different object [43, 44]. Registration process often do have some uncertainties from the input, algorithm, or output, and typically the artifacts are the main source of them. Calibrating the imaging equipment and selecting the most optimal imaging parameters should be taken care of [17], but it is also important to take into consideration patient's changing position, motion, breathing, weight loss or gain, and the possible effects of heart beats at each data acquisition [40, 45].

Rigid and non-rigid object motion analysis algorithms must be applied to get clinically useful system that can analyse sequences and display the estimated results of the given image. Many non-rigid registration methods that are based on 3D geometric features utilize anatomical surfaces [46] and different surface-based registration algorithms can

[2] https://anhir.grand-challenge.org/

typically extract boundary points of interesting structures, match the source and reference surface, and extend the surface-based transformation to the full volume. Non-rigid registration is part of acquisition and reconstruction of images, as well as the postprocessing phase, and it is used to segment structures automatically from the scans. Two decades ago, in a year 2004, it was said that in 21st century a non-rigid registration is likely to become progressively an important component of medical imaging systems [16].

2.3 Staining Sample Tissues

The seen color of stained tissue slides can vary considerably depending on staining conditions in their different environments and the time lapse between slide preparation and scanning [21]. For example, in breast cancer prognosis it is a significant biomarker to observe the H&E histological tissue sections under light microscopy to see the number of mitotic figures per tumor area. WSI and computational pathology both have enabled the development of a new era of automatic mitosis detection algorithms based on convolutional neural networks (CNNs) [47]. Due to non-uniform staining, big number of cells in a small tissue area, and complex and noisy background, it may be challenging to identify specific cells [48]. Recently, there have been new approaches to mimic variations of specific H&E stains. For example, it is said that selecting dominantly stained H&E pixels could be automated by calculating stain vectors for H&E and then use those vectors to derive representative pixels in the future [49].

Samples are processed in many ways before the scanned WSI image is available. Figure 1 shows the process and different phases of tissue's journey from the patient to the whole slide image. After tissue collecting, the sample goes through various phases before pathologists can see the results. Leica Biosystems[3] has described the process thoroughly. Tissue is fixed, cleared, paraffin embedded, sectioned, stained, mounted, scanned, and preprocessed before observing [50]. If the images are processed without preprocessing, the result may cause incorrect diagnosis. Avoiding that, it is important to prepare the images correctly and stain them properly to decrease the problems of color variations [8]. At first, a tissue must be sampled and fixed either paraffin embedding, or through freezing in optimal cutting temperature compound. Usually, the tissue samples are sectioned into thin 2-10 µm slices, labelled and stained, and then mounted on a glass slide. After these phases the sections can be stained by a specific chemical staining protocol that allows identifying histological structures saturated by dyes [35, 51]. In need of multiple stains, multiple tissue sections are cut and separated for each stain. The special stains usually take more effort in preparation and monitoring time, and that increases the cost and time

[3] https://www.leicabiosystems.com/knowledge-pathway/an-introduction-to-specimen-preparation/

spent in the process. H&E staining is executed by using a streamlined staining procedure instead [35].

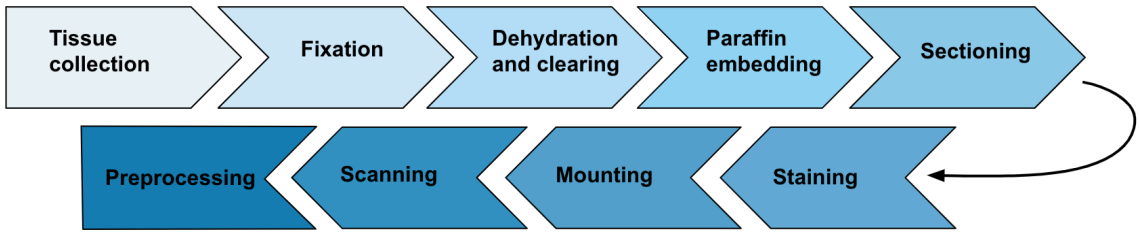

Figure 1. Flow chart of the phases of tissue sample progress from the collection to the digital image preprocessing phase.

Without dyeing the samples look transparent under the microscope. Most of the stains in the images absorb light, and if there is no visible stain in the image, the entire source of the light passes through the tissue and appears as bright white. The areas near the stains are darker in color than those areas without stains [50]. Stain chemicals bind to the tissues and absorb colors from violet to red of the visible light spectrum according to tissue's texture. However, the stained samples can be prone to background illumination or camera change, for example [52]. Also, histological sample preparation and digitization can cause some color variations that may influence the performance of analysis systems' segmentation and classification algorithms. Digitization systems, staining time, and concentration and pH of the solutions have a key role in a successful staining process, to name a few. It is not a coincidence that color normalization algorithms have been developed for color adjustments [2] and it might be the first preprocessing step for any computer-assisted automated diagnostic tool [52]. Figure 2 represents an example of stained tissue slide (a) and tissue microarray microscope (b) that can be used while observing multiple samples simultaneously.

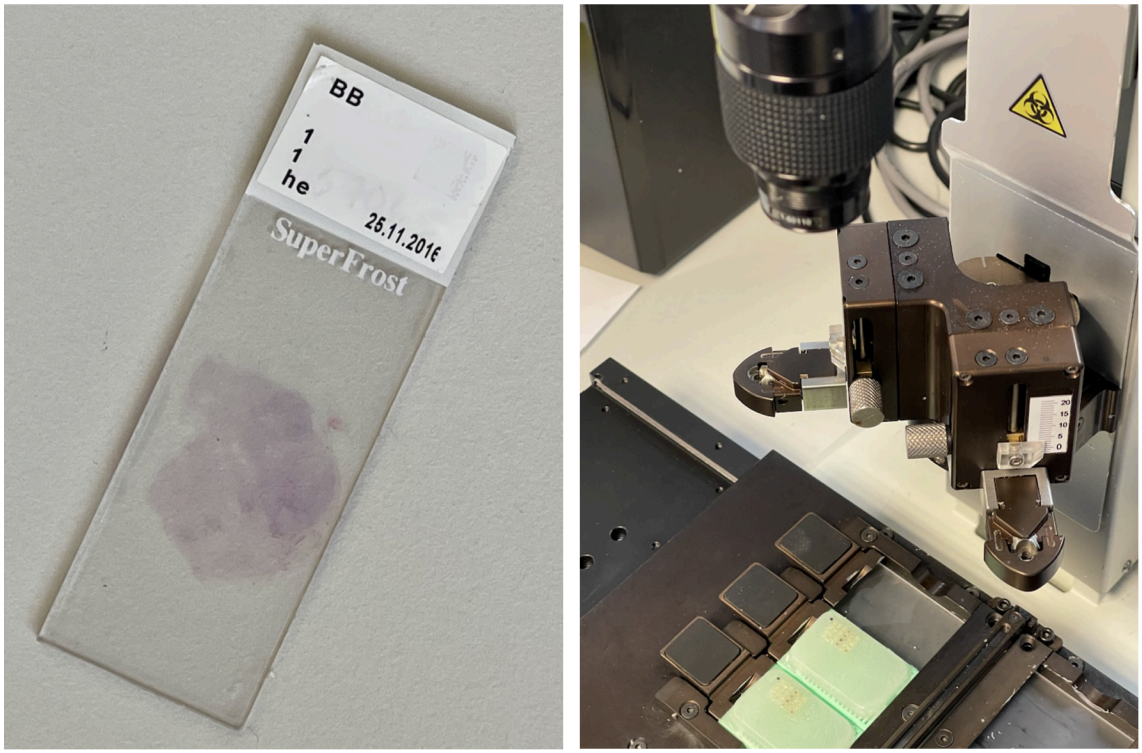

Figure 2. Stained tissue slide (a) and tissue microarray microscope and biopsies in paraffin (b).

2.4 Landmark Validation

In ANHIR challenge [39], the significant tissue structures are marked with landmarks that are divided throughout over the tissue. In ANHIR dataset the landmarks are identified manually for each image and each set has correspondences allowing the validation of geometric registration accuracy between any two images in every set. The landmarks of ANHIR challenge have standard structure of ImageJ software and coordinate frame where the origin is in [0, 0] in top left pixel, more detailed information can be found from their website[4] and git[5]. The simple given landmark example file has a following kind of structure:

```
  ,X,Y
1,226,173
2,256,171
3,278,182
4,346,207
...
```

[4] https://anhir.grand-challenge.org/Data/
[5] https://borda.github.io/dataset-histology-landmarks

Collection of these landmarks is also called annotation. When the annotations are made manually by human, they probably are a bit inaccurate because of the used zooming scale and the possibility that users recognize the tissue structure a little shifted. The challenge presents an additional annotation which goal is to improve the precision of human made annotations. Before every image of the set is annotated, the process goes through the landmark loading and exporting image by image. [39]. Figure 3 is a capture of manually landmarked mammary gland tissue giving an example how the landmarks look like on virtualized tissue. Usually, the performance of registration is measured using distances between the landmarks. In ANHIR challenge the most time-consuming part has been the annotation of the landmarks for provided images. Sometimes there may be wide areas with lack of corresponding structures and hence only few landmarks can be identified. Borovec et al. suggest combining these manually obtained landmarks with other supplementary means to evaluate the quality of registration, which could be done by measuring overlap using reference segmentations or even running synthetically generated deformations [27].

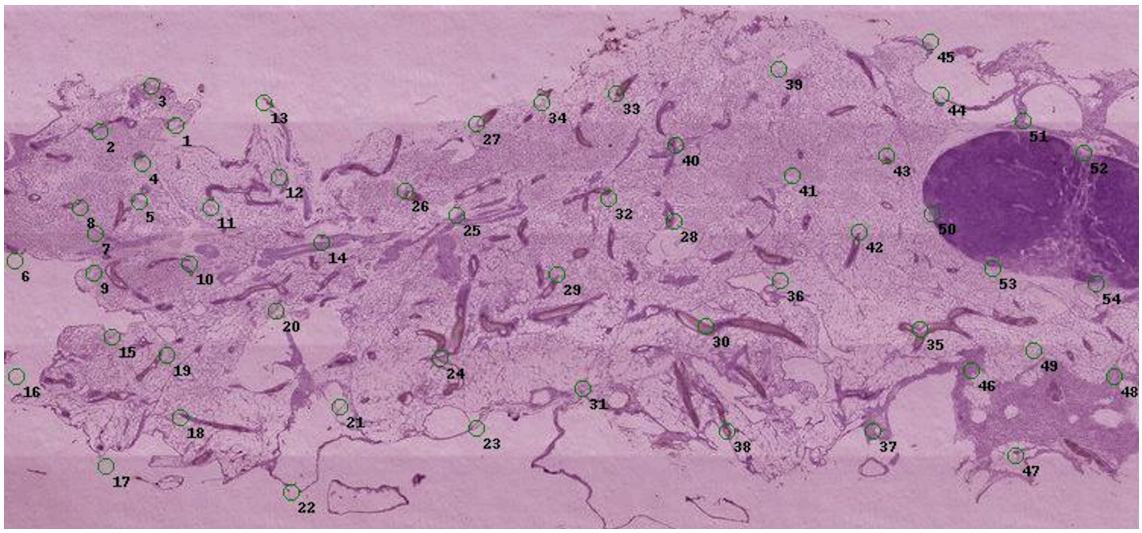

Figure 3. Mammary gland tissue with manually annotated numerical landmarks from ANHIR dataset.

In paper from Noothout et al. [53] they summarize that fast, automatic, and accurate landmark localization methods could help with the precise localization of multiple landmarks, and it also has a possibility to replace manual identification. When classification-based techniques discover the landmark in image patches, slices, or voxels, regression-based methods can predict the displacement or distance to the landmark from them. In the same paper an automatic method for anatomical landmark localization is proposed. It is attached to global-to-local analysis where multiple landmarks' locations are predicted simultaneously by a fully convolutional neural network, and after that, specialized fully CNNs take care of refining the global landmark locations. Regression is used to predict displacement vectors pointing from the center part of the patch to the

landmarks for every patch in the image. In turn, to predict the presence of landmarks in each image patch, classification approach is used. During their research they found that the networks that were trained for multi-landmark localization reached a little better results in comparison with those ones trained only for single landmark localization in Coronary Computed Tomography Angiography.

2.5 Stain Augmentation and Color Normalization

Stain color augmentation, more generally data augmentation, could be a great method to reduce CNNs generalization error by simulating realistic variations of the data used in training process, where the test samples are mimicked by artificial variations. Based on Tellez et al. empirical evaluation, any type of stain color augmentation is highly recommended to be used because without it, all stain color normalization techniques reach poor efficiency. One of their hypotheses says that even in the case of excellent stain normalization method, color information may have a role in a source of overfitting, which in turn impairs suboptimal normalization [36]. Xiao et al. say that the main idea of color augmentation stands for imposing color characteristics from one image to another by using a statistical analysis. It can be achieved by limiting the transformation only to the stained sections of the histological images. In their words, one possible proposition would be a stain-focused image augmentation technique to augment training images using color-matching. The variations of colors in histological images are usually result of stains when the background of the images is bright, and that is why the paper suggests that instead of touching the image background at all, the color transformation should be applied straight to the stains rather than the whole image [54].

Stain normalization allows the data harmonization from several different image modalities showing stain variability. It can be used to upgrade manual examination performance or preprocessing tool for computer-based analysis [24]. Different tissues have different biological factors such as their structure, orientation, functionality and cellular organization, and various staining protocols can cause high visual appearance variabilities depending on each tissue's features [55]. Color normalization process is about minimizing the color variations by realizing color transformation from one image to another one [3]. In one hypothesis [49] the color appearances of two different images would be similar when their color statistics match. Nevertheless, matching the statistics of the whole pixel population of the source and target images can lead unintended artifacts. Tellez et al. found in their study [36] that the best performing method actually did not use any color normalization process, and that finding led them to question if color normalization is a needed tool at all. Overall, the final result of their study is that the high classification performance in histopathology images is possible to achieve without using any color normalization, even though color normalization may help to produce more robust classifiers.

3 WHOLE SLIDE IMAGE PROCESSING

Research laboratories performing tissue-based research, like in biomarker discovery, were one of the firsts to adopt digital pathology due to its high value in multiparametric outputs offered by quantitative image analysis [10]. Digital cameras becoming more common also the area of telepathology was invented helping to tie up the work and analysis of pathologists. The pathologists have a crucial role in the workflow of digital pathology, tissue image analysis, and particularly in the iterative process of algorithm development. They can ensure the quality of stained histology slides as well as the generated data by bringing their technical knowledge of tissue handling, processing, and staining, combined with the specialty expertise in biology, histology, pathology, pathophysiology, biomarker expression, and comparative anatomy [10].

By using AI algorithms in pathology, many of the manual and subjective tasks can become more automated and standardized. Thus, digital pathology together with AI has an immense potential for precision medicine. Even though the automated image analysis is helping the healthcare for example by reducing the misidentification errors, it is very unlikely that those systems could replace completely the full diagnostic capabilities of a pathologist in the near future, and the notion of AI replacing pathologists is just a speculation at this point. [4]. However, this technology can be a helpful supplementary tool in reporting and sharing the process. The computer-assisted safety checks have value in ensuring every slide is reviewed and all core data items are completed in a synoptic report. For sure a combination of an expert and AI will yield results that are more useful, accurate, and consistent than what an expert can do alone, but for now AI is a tool for people in their work. AI is a fascinating application to make decisions in narrow fields but there are still factors that humans can better consider. Human brains are better to synthesize some information than machines would be [4, 11], for example what comes to the ethic decisions.

3.1 Imaging in Pathology Research

Digital cameras nowadays produce still images and microscope-mounted videos that enable the use of live examination of slides, also called as dynamic images. Still and dynamic images can be transferred to remote sites even to the other side of the world, to be then assessed by another pathologist. This procedure is generally called telepathology, and it describes the remote pathology diagnosis using digital image transmission. Comparing to the manual systems, digitalization enables more effective data storage and optimized and standardized visualization and transmission [11, 22, 24]. Human eyes sense colors mostly in three bands that are red, green, and blue and thus pathology images capturing cameras traditionally cover sensors for red, green, and blue lights individually. It is worth of mention that there is a possibility for other wavelength bands have special

information as well. Multiple bands, from three to ten different ones, have been utilized in analysis to develop algorithm execution in image recognition [21, 56]. Pathologists can make the same decisions and judgements on a computer screen that they would do with a traditional microscope, but Snead et al. summarized that there have been results showing the digital image quality at high power would not always be as good as the images obtained with a microscope [13].

In the report of Brock et al. [17] it is mentioned that image registration and fusion algorithms exist in almost every software system that is involved in radiotherapy. Typically X-ray computed tomography is the primary imaging procedure to construct high detailed 3D anatomic and physical models of the cancer patient. These 3D models are in a key role when designing the beam arrangements and shapes, calculating the dose delivered by these beams, and being a guide to locate the patient for treatment [10]. As some previous studies have listed, image registration is commonly used in various analytical research areas to better understand population propensities of phenotypes, estimate tissue changes, and even find out cells or tissues that are affected by the disease [30, 57].

3.2 Role of Deep Learning in Pathology

A machine vision technique searching images by analyzing their content such as color, shape, or texture (rather than only their associated metadata) is now full of new possibilities for opening slide and image archives that have been long held by pathology departments. The main three applications of digital imaging are telepathology, digital pathology and computational image analysis [7]. The modern automated methods provide great support for the basic routine tasks, including counting objects and segmenting regions. On top of that, state-of-the-art machine-learning approaches can reveal the hidden patterns on tissues [58]. Said that, DL has a huge potential not only to decrease the time spent in analysis and decision making but also to enhance the diagnostic accuracy. Maximilian et al. say automated assistance tools to be one of the major topics in the near future [24]. Machine learning and its advantages have enabled the synergy of AI and digital pathology and are now offering image-based diagnosis possibilities that were earlier limited only to the fields of radiology and cardiology. These days the computer-aided diagnostic techniques and advanced algorithms help pathologists to view beyond microscopic slides and share those whole slide images for telepathology and clinical use [4].

Deep neural networks, known also as deep learning, are inspired by the working mechanisms of the human brain. These networks have hidden layers between the input and output, and there are many neurons in each layer. Neurons are also called kernels, usually meaning a mathematical function. Each kernel takes some given inputs and then computes an output. In a study of Wang et al. [21] it is said that in a model of

convolutional neural networks, a kernel computes a feature at a specific location in the input space. Nowadays, the development of deep learning has considerably speeded up pathology image analysis as DL models and algorithms can optimize an enormous number of given parameters (inputs), considering histology images' high-resolution. They have summarized that traditional image processing methods face difficulties in staining and lighting conditions [32] while the models utilizing DL mostly use data augmentation to overcome that problem [59].

Not only are the pathological images huge in their size and resolution, but also they are coupled with large and complex deformations. The main challenge of these DL methods is large GPU (Graphics Processing Unit) memory utilization while computing the tasks with these memory eating whole slide imaging files. Downsampling is suggested to be the simplest solution what comes to saving GPU memory, and that approach was used to apply volume of network during the ANHIR challenge too. Nonetheless, the downside of downsampling is its tendency to reduce registration quality and thus make it harder to register fine image details [27, 28, 60]. Medical pictures typically have some noise, little tissue contrast across organs of interest, and they may require 3D image modification to be more readable. What comes to paper of Salehi et al. one of the most challenging tasks in the deformable medical image registration problem is the creation of ground-truth data to train the deep learning models in fully supervised transformation estimation. Unfortunately, a dense flow field ground-truth correspondence is rarely available [61]. Most of the computational time in DL registration is directed on training process as it can practicable be done offline using a server reserved for machine learning. Being crucial to clinical practice, deep learning permits a real-time non-rigid registration. The registration accuracy is close to the level of human made annotations. Still, the system's computational time is relatively high, and that limits its use in clinical environment [28]. In another study [9] it is claimed that it is very challenging in computational approaches to mimic the ground truth annotations done by expert, as it involves outlining object boundaries and annotating pixels corresponding to an interesting region or tissue.

Advantages of deep learning algorithms include highly parallel GPU-aided computation that enables classifying or segmenting a 1000 × 1000 pixels image in less than a second. Also, the flexibility of neural network structure consisting of loss function selection and framework designation is a great benefit. Such a network is trained by minimizing the loss function, that is known as a measure of the separation between ground truth and prediction. There are some popular neural network frameworks called Keras[6], TensorFlow[7], and PyTorch[8]. DL methods are utilizing image data to its fullest as the prediction model can take advantage of all the pixels, and CNN models are robust to

[6] https://keras.io/
[7] https://www.tensorflow.org/
[8] https://pytorch.org/

various staining circumstances in analysis of pathology image [21]. The challenge in deep learning approaches is the need of huge amount of labeled training data, and large files usually take lot of time to compute [24].

3.3 Utilization of AI and ML

Developments of AI motivates pathology to rapidly transition to digital methods [4]. Digitalization offers new ways to use tools only pathologist have operated in the past. It is said [7] that nowadays also the individuals having no deep experience in machine learning techniques can benefit from machine vision in a field of pathology. Earlier, only highly skilled pathologists were able to identify the existence of tumor cells in a small, dissected tissue area, its being laborious and time consuming. With the help of computer-aided automatic detection tools, the false negative rate and subjective bias can be widely reduced and that is a key for better early detection and treatment, improved accuracy, and quicker examination process [21, 62].

Combination of AI and digital pathology enables research teams instantly to share and review the pathological images and take advantage of computational algorithms to evaluate new visions that could otherwise be ignored due to their hidden data. Those valuable insights can eventually bring more information and hence lead to the more detailed cancer diagnosis. In its best, this integration can produce more personalized care plans for each cancer patient [4]. Anyway, computer-aided diagnosis is still seen as one of the most demanding challenges in medical image processing field [63]. AI has a possibility to be an important assistant in a quality assurance as it can provide quality checks and apply automated diagnostic algorithms on the diagnosis. It can also serve improved solutions for out-of-focus area detection or color augmentation and normalization [4]. Models of AI, ML, and DL, can all be used for many types of purposes in disease diagnosis, involving segmentation, automatic detection, and quantification of structural changes and histological parameters [7]. Basically, ML and pattern recognition manage the problem of automatically finding a decision from many different option pools, like in separating tasks. Detection and recognition are there for helping to detect some certain element in huge medical images where efficient parsing is required [63]. An artificial neural network is described as a non-linear statistical data modeling tool that is used to find patterns in data or to model complex relationships between given inputs and outputs, for example. It is a mathematical or computational model inspired by biological neural networks and during the learning process it changes its structure based on internal or external information flowing through the network [15].

3.4 Overview of Registration Methods in ANHIR Challenge

In this section some of the registration methods of former studies are presented shortly. All the following techniques were introduced in ANHIR challenge by Borovec et al. [27] where these registration techniques were used with the same settings and the same image pairs.

AGH method from the team AGH UST [64], converts the images to grayscale before downsampling and histogram equalizing them. It applies various approaches before automatically selecting the best result of them based on a similarity criterion. Rigid transformation or an initial similarity is determined by Random Sample Consensus from feature points that are detected by the techniques of Scale-Invariant Feature Transform (SIFT) [65], Orientated FAST and Robust BRIEF (ORB) [66], or Speeded-Up Robust Feature (SURF) [67]. The initial transformation takes care of the situation in case of failure as it aligns binary tissue masks that are calculated from the images. A non-rigid transformation uses local affine registration or a feature-point-based thin-plate spline interpolation. Borovec et al. found one of the most effective procedures to be the MIND-based version of Demons algorithm. **CKVST** method from Chengdu [68], is about decomposing the images into three separate channels by a procedure of stain deconvolution, and it uses only the hematoxylin-stained channel. A rigid transformation is refined by evaluating the similarity on a selected high resolution patches' set. A non-rigid registration can be found locally, represented by B-splines. Both the rigid and non-rigid registrations are using the normalized cross correlation with gradient descent and limited-memory optimizers. **TUB**, University of Tsinghua [69], uses a combined standard deviation for all color channels. For subsequent registration, a scalar feature of $\sigma = 1$ pixel is used. The size of used image is reduced to 512×512 pixels or so, and then padded to keep the aspect ratio. A rigid transformation is estimated before a dense non-linear transformation in this technique. The used network is trained with an unsupervised manner to maximize an image correlation coefficient, and after that, it is fine-tuned by using the positions of provided landmarks on the training data. **TUNI** is a method from University of Tampere [70] where the images are first converted to grayscale and then histogram equalized by CLAHE (Contrast Limited Adaptive Histogram Equalization). The registration uses Elastic Stack Alignment to find a rigid transformation by using Random Sample Consensus from SIFT features. To keep the transformation close to a rigid registration, a non-linear registration uses a normalized correlation and virtual springs. **UA**, University of Alberta [71], rescaled the images to 1/40 of their normal size and then converted them to grayscale. The order of estimation is from a translation and rotation to a non-rigid registration that utilizes a moving mesh framework. Its idea is to alternate the correction steps imposing incompressibility and gradient descent on densely represented deformation, where the both steps are using a mutual-information similarity criterion.

Also, some well-known and generally used registration methods were represented in the study. Summarizing the methods, it can be said, that **Elastix** [72] is a software that provides a command-line interface that is simple to use while operating the Insight Segmentation and Registration Toolkit. B-spline deformation and MI similarity criteria with the adaptive stochastic gradient descent optimizer were used in this method. **NiftyReg** [73, 74] software performs a block matching based affine registration and a B-spline non-linear registration. **RVSS** is an abbreviation of Register Virtual Stack Slices and it is an ImageJ software registration plugin extending the bUnwarpJ method, and it incorporates also SIFT feature points to add robustness [65, 75]. A rigid transformation was refined using a B-spline transformation during the research of Borovec et al. [27].

3.4.1 Registration Techniques in Literature

A fundamental task of registration is to match at least two images together which are possibly taken at different times from different viewpoints or sensors. The systems using image registration as a main component are used as target recognition by matching a target with a real-time image of a scene, monitor of global land usage using satellite captures, and especially align images from various medical modalities that is an important aspect in digital pathology. Common problem is that images taken at different viewpoints or several angles need to be comparable so that the points of the images relate to their corresponding points. One way to detect the differences is to align images to one another and the proper alignment between the images have to be found [76]. There are techniques to compute deformations, match features and keypoints, and utilize tissue surfaces, for example. The process is non-linear, deformable, when the estimated transformation does contain rigid transformation such as translation or rotation but also deformations like shrinking or stretching. Deformable image registration includes geometric transformation between two images mapping them both onto a common coordinate system [45].

WSI registration fusing the information from several neighboring immunohistochemically stained slides is proposed in research of Lotz et al. [77]. The idea is to use a non-linear deformation model to register the images with a low resolution and then refine the outcomes on patches by using a second non-linear registration. On each patch, the deformations are computed to merge the interpolation of one globally smooth non-linear deformation. Ziaul et al. propose a gradient computational registration system that contains a robust keypoint matching algorithm. Its benefit is a combination of scale, keypoint orientation, and position that can increase the correct keypoints' matching number which then makes the method robust in transformation of complex non-linear intensity. There are also many classical methods that can match features effectively such as KAZE [78], ORB [67], SIFT [68], SURF [69], to name a few [30]. Registration algorithm can basically be decomposed into components of the similarity measure of two images matching and the transformation model that specifies how the source image could

change to better match the target image. Combining both geometric and intensity features in registration leads more robust methods. In geometric registration anatomical information is used over some parts of the images while intensity-based registration focuses on matching intensity patterns over the entire image, without the anatomical knowledge [16].

The area of image registration is wide and contains many use cases also outside of the field of digital pathology. Image registration is a crucial tool in digital pathology, but also provides great ways to work in industries such as food, agriculture, military, defense and security, robotics, and satellites as well. Some examples of the image registration techniques are briefly described to give an overview of the literature. For example, a hybrid deep feature-based deformable image registration framework is proposed for stained tissue samples in a paper by Zhang et al. After extracting dense feature points, they performed points matching by two deep learning feature networks. Their proposition is an outlier detection method that combines isolation forest statistical and the local affine models for further decreasing false matches. In conclusion, the interpolation technique produces the deformable vector field that is then utilized in image registration based on the matching points [20]. The hybridized negative transformation algorithm uses negative or inverse transformation that is linear gray level transformation. The linear transformation function maps pixel's gray level value into different gray level at the same position and its benefit is specially to help finding the interesting details from the processed panoramic images [79].

A surface method is an image registration technique where the boundaries or surfaces are often more observable than landmarks and that is why Wyawahare et al. propose them to be used for segmentation by locating high contrast borderlines and surfaces. The image having higher resolution or covering larger volume of the patient is used when generating the surface model [15]. Szeliski and Shum represent cylindrical panorama built from a sequence of images and image mosaic by a set of transformations in their paper [80]. All transformations correspond to an image frame in the sequence of input image and then represent the mapping between image pixels and all viewing directions. Once the complete panoramic mosaic is constructed, input image set and associated transforms need to be converted into images that are quick to view. In an overview of Wyawahare et al. [15] there are many more techniques presented, such as Curve methods, Moment and Principal Axes methods, Correlation methods, Atlas methods, and Wavelet-based methods.

3.4.2 Image Registration Steps

According to survey from Zitová and Flusser [81] and to overview of Wyawahare et al. [15], the most of image registration methods contain the following steps. The steps are illustrated in the figure 4 that represents some example landmarks on myoma tissue.

- **Feature detection**: Pronounced objects, such as edges, outlines, corners, or closed-boundary regions are detected (manually or automatically). The same features can be presented by their control points like the centers, line endings or distinctive points.

- **Feature matching**: The correspondence between the features in the sensed and the reference image are established. Similarity measures and feature descriptors are used in this step.

- **Transform model estimation**: The so-called mapping function's type and parameters of the sensed and reference image are estimated, and the parameters are computed accordingly the established feature correspondence.

- **Image resampling and transformation**: The sensed image is transformed with the help of mapping functions. Non-integer coordinates image values are computed by some interpolation technique.

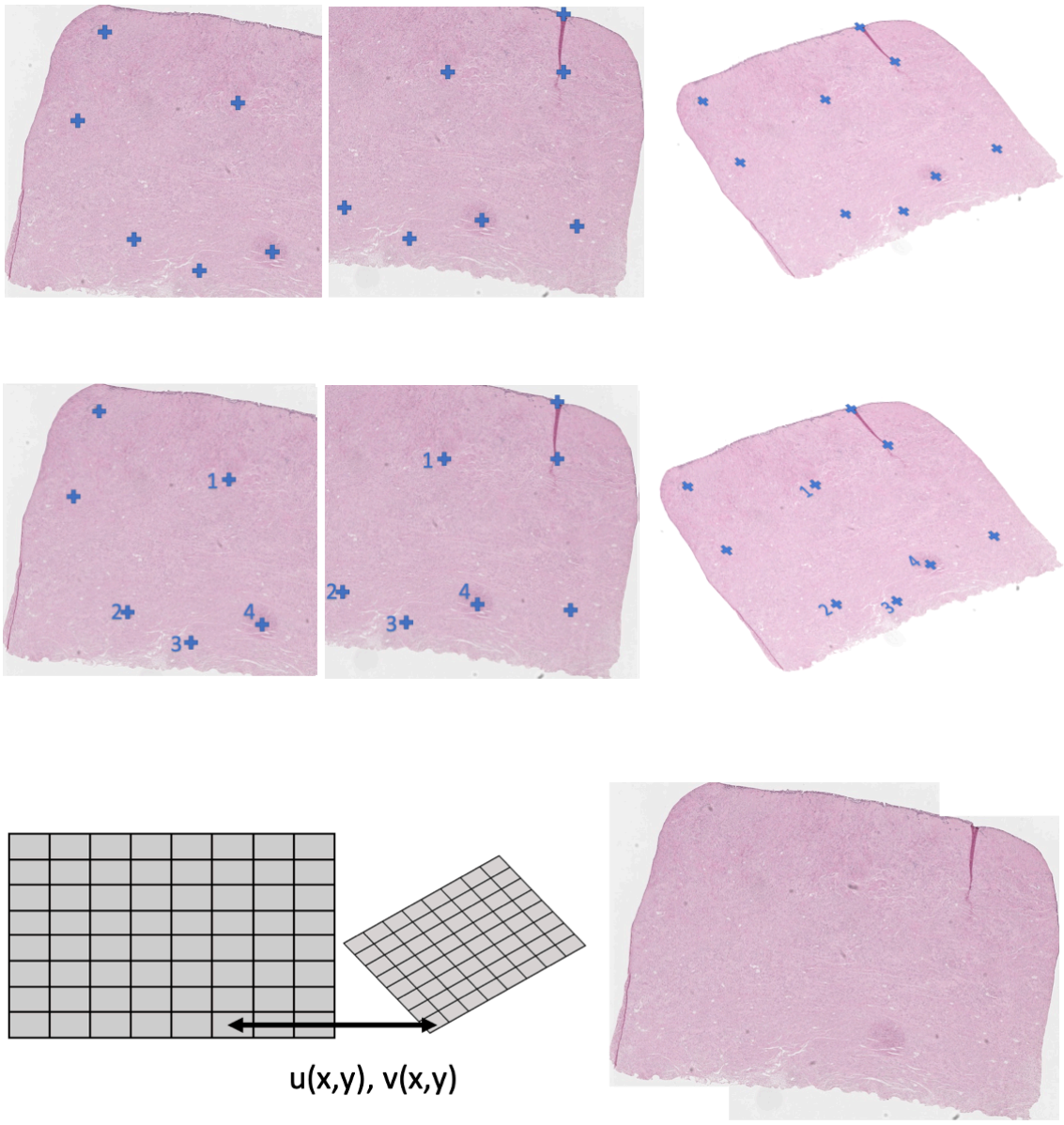

Figure 4. Image registration steps. Feature detection of random abnormalities (top), feature matching by the corresponding pairs (middle), transformed model showing the correspondence (bottom left), and image resampling and transformation using interpolation technique (bottom right), inspired by Zitová and Flusser.

4 METHODS

The preparation of tissue slides is different for each dye as the sample slides are deformed and before further processing a non-rigid registration is required. There is still complexity in registration of histology images such as a high resolution, large file size, non-rigid deformations, diversity in the appearance and partly missing data in consequence of the multiple dyes' usage [38]. In research of Borovec et al. they found that the hybrid methods which combine both feature- and intensity-based criterion are accurate and robust [14].

4.1 Materials and Tools

Myoma and ANHIR datasets are used in this work. The whole slide images are handled in .SVS format which requires a specific tool to open as an image. In fact, .SVS format means a file that is an image in Tiled Tagged Image File Format and has some additional images including the overview image, slide label, and some smaller scaled copies of the scanned image. Tagged Image File Format enables file storing and it has a support for compression with its multiple tiled images. With the tiled format it is possible to load and display the large high-resolution images by loading only the tiles that are necessary at the time. WSIs indicate any format of image that also includes a Region of Interest scanned from microscope slides. The traditional file formats would have too low limits on image dimensions to be used for whole slide image purposes [88].

4.1.1 Myoma Dataset

Collection of myoma tissues is approved by the ethical committee of the Northern Ostrobothnia Hospital District. The dataset consists of 20 H&E stained Leica Aperio images of myoma tissues in .SVS format and there is four parts to be processed in each image. The myoma collection is used in former research of Physiological Signal Analysis Group at Center for Machine Vision and Signal Analysis in the Faculty of Information Technology and Electrical Engineering at University of Oulu, Finland. The samples have been digitalized using Leica Aperio AT2 whole slide scanner. Table 1 shows information of two scanned whole slide images to give an example of the image details of myoma tissue. Image 1 opened on Aperio ImageScope can be seen below in figure 5.

Table 1. Details of two whole slide images of myoma tissues, scanned by Leica Aperio AT2 scanner.

Feature	**Image 1**	**Image 2**
Description	Aperio Image Library v12.0.15, 101 600 × 50 382	Aperio Image Library v12.0.15, 99 568 × 59 004
Apparent Magnification	40×	40×
Image Type	SVS/JPEG 2	SVS/JPEG 2
Image Width	99 600 pixels	97 608 pixels
Image Height	50 282 pixels	59 004 pixels
Image Depth	1 pixel	1 pixel
Image Channels	3	3
Image Bit Depth	8 bits	8 bits
File Size	2 132 093 000 bytes	2 180 541 000 bytes
Compression Type	JPEG using libjpeg	JPEG using libjpeg
Compression Quality	70	70
Compression Ratio	7.05	7.15
Tile Width	240 pixels	240 pixels
Tile Height	240 pixels	240 pixels

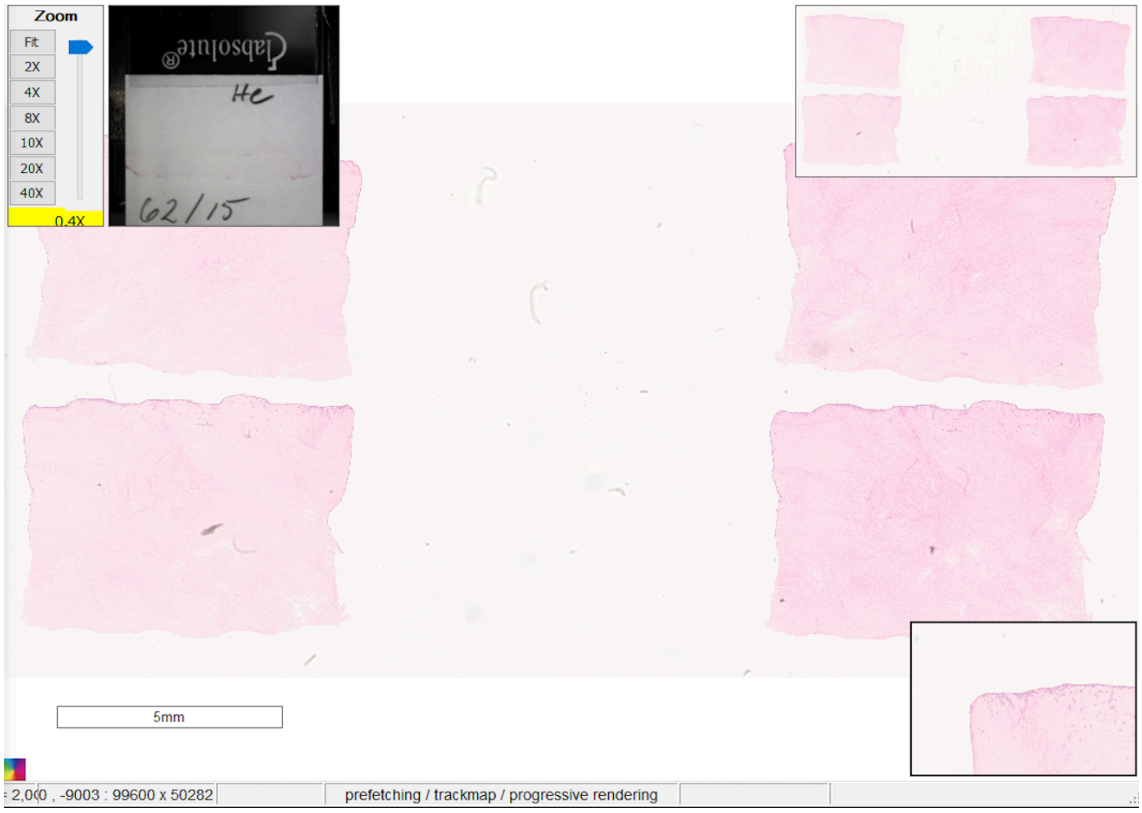

Figure 5. Myoma tissue observed on Aperio ImageScope.

Nurmenniemi et al. [82] concluded myoma tissues mimicking the native tumor microenvironment better compared to organotypic models from previous studies. This improved organotypic culture model provides a potential tool to analyze the carcinoma cells' behavior and it bases on human myoma tissue. The idea of the model is to study the behavior of cancer cells in environment that mimics the situation of reality. Myoma has a role in modeling the real situation while cancer cells are set on top of it. It was seen that myoma does enhance the invasion depth of several human cancer cell lines originating from various tissues.

4.1.2 ANHIR Dataset

The dataset of ANHIR tissues consists of high-resolution whole slide images of different kinds of tissues such as breast, kidney, gastric, lesions, COAD (Colon Adenocarcinoma), lung-lobes, and mammary-gland. The images are up to 40× magnification, and the original image size ranges from 15k × 15k even up to 50k × 50k pixels. The whole slide images are organized in consecutive tissue slice sets where all the slices cut from the same tissue are stained by different dyes. Table 2 contains information of the WSIs from ANHIR challenge. The dataset is made available under the license CC-BY-NC-SA [39]. Since the dataset of ANHIR challenge is public, testing the different methods and reproduce the received results is accessible for everyone [28].

Table 2. Details of ANHIR dataset tissues scanned by different WSI scanners.

Tissue	**Scanner**	**Magnitude**	**Resolution [µm/pixel]**	**Avg. Size [pixels]**
Lung Lesion	Zeiss Axio Imager M1	40×	0.174	18k×15k
Mice Lung Lobes	Zeiss Axio Imager M1	10×	1.274	11k×6k
Mammary Glands	Zeiss Axio Imager M1	10×	2.294	12k×4k
Mice Kidney	NanoZoomer 2.0HT	20×	0.227	37k×30k
COAD	3DHistec Pannoramic MIDI II	10×	0.468	60k×50k
Gastric Mucosa	Leica Biosystems Aperio AT2	40×	0.2528	60k×75k
Human Breast	Leica Biosystems Aperio AT2	40×	0.2528	65k×60k
Human Kidney	Leica Biosystems Aperio AT2	40×	0.2528	18k×55k

Each sample of consecutive tissue slices is differently stained, and the dyes' names can be found from table 3 where also their characteristic hue is mentioned if available.

Figure 6 illustrates the virtual tissue slides of human breast, mice kidney, and human gastric with different stains.

Table 3. Names, abbreviations, and the common hues and usage of some stains used in ANHIR challenge.

Stain name	**Abbreviation**	**Color**	**Usage**
Antigen KI-67	Ki67	Red	Proliferating mammalian cells
Clara cell 10 protein	Cc10	Brownish	Lung, lesion
Estrogen receptor	ER	Brownish	Breast
Hematoxylin and eosin	H&E	Purple, pinkish	Nucleus, cytoplasm
Human epidermal growth factor receptor 2	c-erbB-2 / HER-2-neu	Fluorescent red	Breast, gastric
Periodic acid-Schiff	PAS	Red, magenta	Mucopolysaccharides
Platelet endothelial cell adhesion molecule	PECAM-1 / CD31	Blue	Blood vessels, cytoplasm, histiocyte
Progesterone receptor	PR	Brownish	Breast, uterus, brain, central nervous system
Smooth muscle actin	SMA	Orange, pink	Mammary carcinoma, lymph node metastasis, collagen
Epstein-Barr virus	EVB	Purple	Tonsils, lymph node

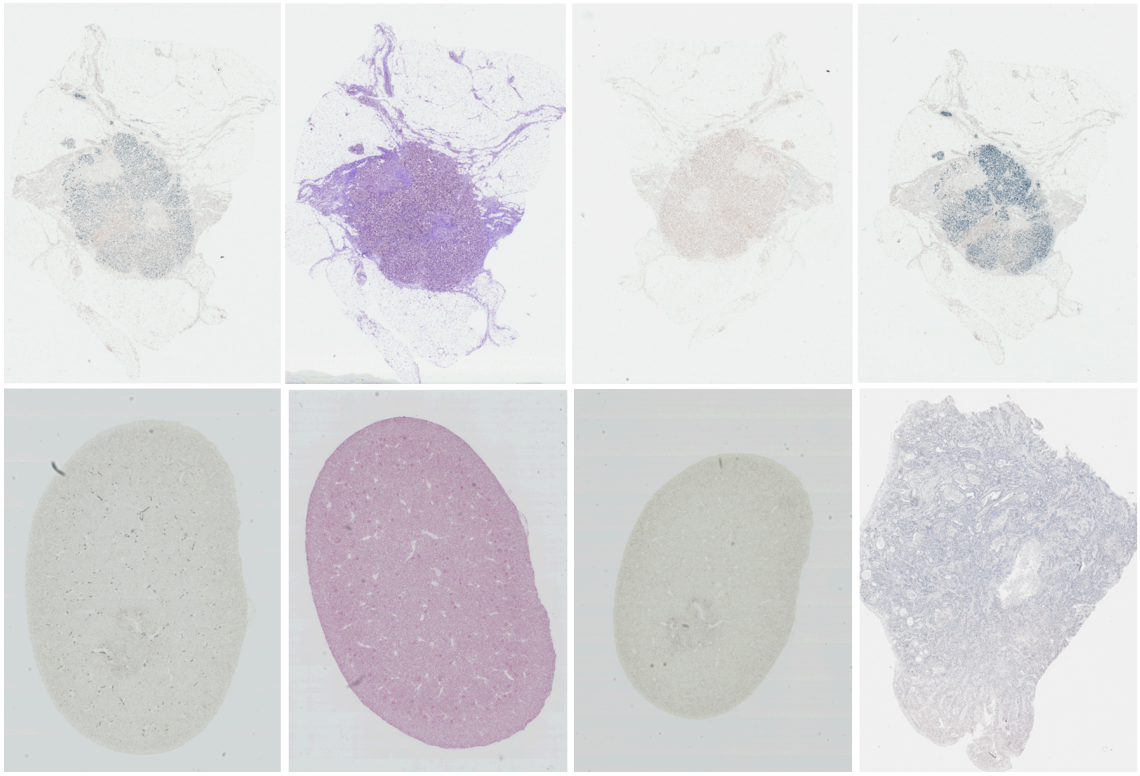

Figure 6. Differently stained breast (top), mice kidney (bottom left), and gastric (bottom right) tissues. Stains from the top left to the down right are called as ER, H&E, HER2, PR, SMA, PAS, CD31, and EBV.

4.2 Unsupervised Deep Learning Registration Framework

The development of proposed method is based on DeepHistReg algorithm [28] with modifications implemented and tested in this thesis. The primary step of stain color feature augmentation contains two main phases which are stain separation and stain color augmentation. The first phase involves extracting color characteristics from WSIs of different domains. This method calculates matrices for stain color and density maps for each domain. These matrices are used in the second phase to improve training images in an unsupervised manner [83]. This is achieved by randomly selecting two whole slide images, I_i and I_j, and breaking them down into their color and density components, M_i, M_j, D_i, and D_j respectively using Beer-Lambert law [84].

$$B = -log\frac{I_{RGB}}{I_o} = MD \tag{1}$$

where I_{RGB} presents a whole slide image in the RGB color space and I_o is the illuminating light intensity. The stain color matrix, M, represents the color appearance of stains in the image. The density of each stain is shown by the density map, D. The mixed stain color matrix, M_{ij}^*, is generated by linearly interpolating between $\mathrm{M_i}$ and $\mathrm{M_j}$. The interpolation coefficient α_i is randomly chosen from a uniform distribution as described below,

$$M_{ij}^* = \alpha\, M_i + (1 - \alpha_i)M_j \tag{2}$$

where $\alpha_i \sim U(0,1)$. By using random interpolation between stain color matrices, the variety of stain color appearances is enhanced. To simulate changes in color fading and stain concentrations, the stain density map, D_i, is determined as follows,

$$D_i^* = rD_i \tag{3}$$

where $r \sim U(1 - \lambda, 1 + \lambda)$ and the scaling factor r, is randomly chosen from a uniform distribution that is controlled by λ, where $\lambda \in [0,1]$. Eventually, the augmented image, I_{ij}^* is generated as follows,

$$I_{ij}^* = I_o \exp(-M_i^*\, D_i^*\,) \tag{4}$$

In the second step some modifications are examined with DeepHist Registration method. The main target of our proposed modifications and DeepHistReg algorithm combination is to find the best feature points to match for registering process. DeepHistReg framework has pipeline including the steps of data loading, data loading, transferring to GPU, preprocessing, initial alignment and feature matching, affine registration, and finally nonrigid registration.

Throughout the registration process, the cost function employed is the negative normalized cross-correlation, N. Global the negative normalized cross-correlation is utilized for initial alignment and affine registration, whereas patch-based the negative normalized cross-correlation is applied during nonrigid registration. Additionally, we incorporate the curvature, C as the regularization term specifically for nonrigid registration similar to the proposed method [28].

$$F(L, R, v) = -N(L, R) + \alpha C(v) \rightarrow min \tag{5}$$

where N represents either the global or local version of the normalized cross-correlation, depending on the specific step being examined. C represents the curvature regularization used solely in nonrigid registration. Parameter α controls the smoothness of the deformation. L, R, and v refer to the warped subject image patches, target image patches, and displacement fields respectively.

The visualization of the framework of proposed unsupervised deep learning registration framework can be seen in figure 7. The main steps of DeepHist registration technique are described in detail below.

• **Preprocessing**: This step includes offline and online stages. All of the image pairs are padded and parsed from the formats of .jpg or .png into uncompressed .mha form to make data loading speeded up. This step decreases the time used in training and inference of data loading process. At first, the pipeline begins from image pair loading, and then converting the pair to grayscale and transfers them to GPU memory. Images are downsampled so that the resolution gets relatively low, 512 pixels for instance, in a smaller dimension. This downsampled pair is used during the steps of background segmentation, initial alignment, and affine registration because the lower resolution seems to decrease the registration time and the higher resolution is not mandatory in these steps.

• **Background segmentation**: The tissues are efficiently segmented from the background using a U-Net-based network [85] as deep segmentation is robust, fast, and easily convertible to other histology datasets, and the computational time only takes a few milliseconds. Segmentation notably improves the registration results of the image pairs having any background artifacts.

• **Initial alignment**: This step contains of calculation of the source and target centroids and translation of the source by the translation vector between the centroids. Then, an exhaustive rotation angle is searched, and the source is warped for each angle and the negative normalized cross-correlation, *N*, is calculated. The chosen angle will be the one with the lowest negative *N*. The compilation of the centroid translation vector and the rotation matrix creates the final rigid transformation. Even though the initial alignment

may not be deep learning based, it uses GPU to lower the time of registration. This step is crucial for cases misaligned by 180 degree rotation.

• **Affine registration**: Convolutional neural network, similar to a ResNet architecture [86, 87], is used in this phase, and the network output is an affine transformation matrix (2×3) that is converted to the transformation grid. The network is trained by optimizing a cost function based on *N*. In the end, the dataset is augmented by random affine transformations applied randomly to the pair of the source and target images.

• **Non-rigid registration**: Because of the GPU memory is limited and the network parameter gradients do not fit into it, a pyramid-based, patch-based, group-based, and iterative deep registration solution is proposed. The procedure of non-rigid registration starts with resolution pyramids which are built for the source and target images both. The iterations of image registrations are started with the lowest resolution. The source image is warped operating the current deformation field and then the images are unfolded into overlapping patches, being still split into smaller groups with predefined size in every development round. Corresponding groups are being distributed through the registration network, calculating the current velocity field that is then concatenated and folded back into the same shape as the current deformation field. After all this, the current level deformation field is upsampled again to the next resolution. After the highest resolution, the current deformation field becomes the final deformation field. However, the number of pyramid levels ensures deformations can be adequately represented by the chosen patch size. Iterations per level increase accuracy but also computation time where the regularization parameter controls the smoothness of deformations.

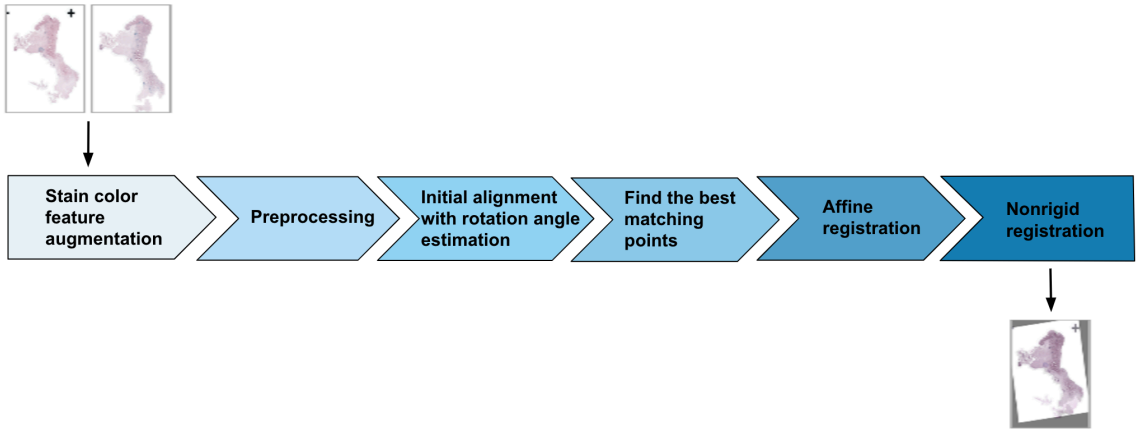

Figure 7. Flow chart of the stain color feature augmentation and matching based unsupervised deep learning registration framework for differently stained histopathology images.

The non-rigid registration method has various parameters such as the size of patch or group, stride, number of pyramid levels and iterations per level, and the regularization parameter that is controlling the smoothness of deformation. These parameters take care

of required receptive field and GPU memory and ensure that the patch size can capture the large deformations. The quantity of iterations in each level defines the amount of times when the patches pass through the network with all resolutions. In pyramid-based approach the images are being registered at different resolutions, from the lowest level to the highest. As in the iterative methods, after the pyramid level the deformation fields are calculated and then upsampled to the resolution of the next level. Patch-based approach means that the images at a given resolution are unfolded into several smaller patches managed by a deep network relatively small. In group-based solution only small groups of patches are transmitted by the network simultaneously due to GPU memory restrictions. Also, the loss function is evaluated and optimized in this level instead of image level. Eventually, the method is iterative as long as the images at each pyramid level are propagated several times through the network, finally increasingly compiling the calculated velocity fields [28].

4.3 Performance Evaluation Metrics

The comparisons of different evaluation metrics measuring the registration performance are calculated by the formulas of Pearson Correlation Coefficient (PCC), Structural Similarity Index Metric (SSIM), Feature Similarity Index Metric (FSIM), Root Mean Square Error (RMSE), Target Registration Error (TRE), and relative Target Registration Error (rTRE). The PCC formula is defined as follows,

$$PCC = \frac{\Sigma_i(x_i - \mu_x)(y_i - \mu_y)}{\sqrt{\Sigma_i(x_i - \mu_x)}\sqrt{\Sigma_i(x_i - \mu_y)}} \tag{6}$$

where x_i and y_i are the symbols for the reference and the registered image, and μ_x and μ_y are their respective means. If the coefficient value of PCC lies between ± 0.50 and ± 1, it is said to be a strong correlation. The formula for $SSIM$ is calculated as,

$$SSIM(x, y) = S_1(x, y)S_2(x, y) \tag{7}$$

where x is the reference image and y is the registered image, and S_1 and S_2 are denoted as,

$$S_1(x, y) = \frac{2\bar{x}\bar{y} + c_1}{\bar{x}^2 + \bar{y}^2 + c_1} \tag{8}$$

$$S_2(x, y) = \frac{2s_{x,y} + c_2}{{s_x}^2 + {s_y}^2 + c_2} \tag{9}$$

where $\bar{x}$, $\bar{y}$, ${s_x}^2$, ${s_y}^2$, and $s_{x,y}$ represent the local mean of x and y, the local variance of x and y, and the local covariance between x and y, respectively. The $SSIM$ values range between 0 to 1, and the value 1 means a perfect match between the reconstruct image and the original one. The formula of $FSIM$ can be calculated as follows,

$$FSIM = \frac{\Sigma_{x\in\Omega} S_L(x) \times PC_m(x)}{\Sigma_{x\in\Omega} PC_m(x)} \tag{10}$$

where Ω denotes the whole spatial domain, $S_L(x)$ is a similarity score and $PC_m(x)$ is the phase congruency measure defined as,

$$PC_m(x) = \max\big(PC_1(x), PC_2(x)\big) \tag{11}$$

where $PC_1(x)$ and $PC_2(x)$ represent the phase congruences. The similarity score is the product of similarity measures for phase congruency $S_{PC}(x)$ and similarity measure of gradient magnitude $S_G(x)$ described as follows,

$$S_{PC}(x) = \frac{2PC_1(x) \times PC_2(x) + T_1}{{PC_1}^2(x) \times {PC_2}^2(x) + T_1} \tag{12}$$

$$S_G(x) = \frac{2G_1(x) \times G_2(x) + T_2}{{G_1}^2(x) \times {G_2}^2(x) + T_2} \tag{13}$$

where G_1 and G_2 are gradient maps of the images and T_1 and T_2 positive constants defined based on image properties. Finally, $RMSE$ is defined as,

$$RMSE = \sqrt{\frac{1}{n}\sum_{i=1}^{n}(x_i - x_i')^2 + (y_i - y_i')^2} \tag{14}$$

To calculate TRE, the Euclidean distance is measured between the annotated (arbitrary point) and transformed landmarks (true position of arbitrary point and its registered position). TRE describes the difference between the mapped positions as corresponding points, and the formula is defined as,

$$TRE = Ax_1 + s - (\bar{A}x_1 + \bar{s}) \tag{15}$$

where A and s are the registration transformation parameters whereas $\bar{A}$ and $\bar{s}$ are their respective estimators. The illustration of TRE, inspired by Cohen et al. [89], can be seen below in figure 8.

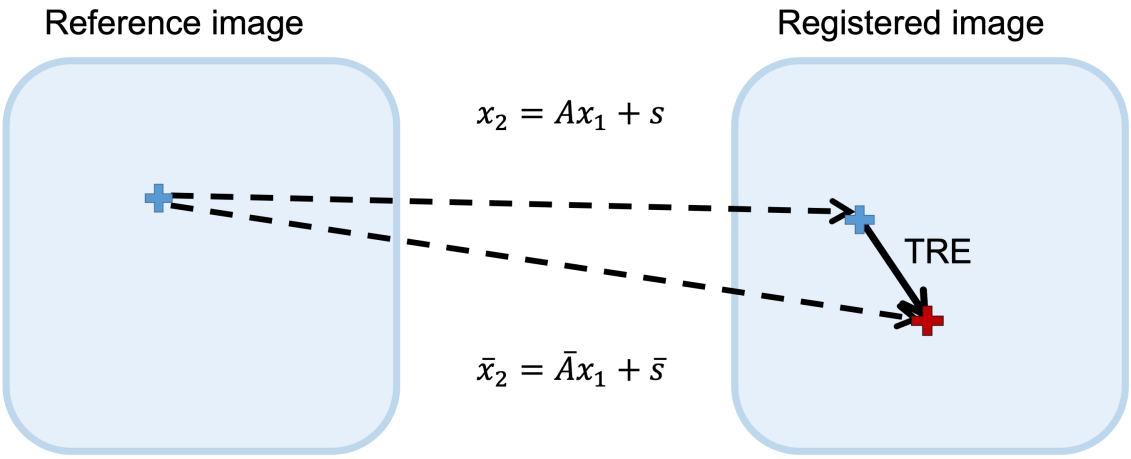

Figure 8. Illustration of target registration error. Reference image having an arbitrary point as the annotated landmark, and registered image containing the true position of the landmark (blue cross) and its registered position (red cross).

TRE can be normalized by the image diagonal to make the registration error comparable between image pairs having different resolutions. That is called relative Target Registration Error and it is defined as follows,

$$rTRE = \frac{TRE}{\sqrt{W^2 + H^2}} \tag{16}$$

where, W and H denote the image width and height respectively. Different rTRE-based metrics are used in this work and they are called average rTRE, median rTRE, and Max rTRE. These formulas above cover up the metrics used in this study when evaluating the stain registration algorithm results. The algorithm calculates the metrics for each whole slide image in the used datasets and prints the results into a list (on Matlab) or into a .csv file (on command line).

5 RESULTS

This study introduces an unsupervised deep learning registration method for high-resolution whole slide image registration and compares the proposed method with state-of-the-art from previous studies. The quality of the proposed method is validated by the metrics of PCC, SSIM, FSIM, RMSE, and rTRE. Also, the visual valuation was used while studying the differences in between the WSIs on landmark-based evaluation. The robustness was evaluated comparing the differently stained images to the registered output image. rTRE was calculated by utilizing manually annotated landmark images from ANHIR and myoma datasets.

The ANHIR data is public and hence it is possible to reproduce the tests in future studies. The proposed method is based on the DeepHistReg algorithm and the same public parameters were used in this work. Some modifications were done on our method and they had a positive impact on the results as can be seen in table 5. The results are presented in tables and figures below. The following evaluation results in table 4 are organized by the highest correlation and SSIM values and the lowest RMSE values. After computing each metric per each image, the code searched for the conditions of $-0.5 < PCC > 0.5$, $SSIM > 0.7$, and $RMSE < 0.1$.

Table 4. Evaluation metrics of registered images having the best values from ANHIR and myoma datasets.

Tissue	**Evaluation metric**			
	PCC	**SSIM**	**FSIM**	**RMSE**
Mice kidney 1 (PAS)	0.8779	0.8716	0.9267	0.0367
Lung lobes 1 (SCP)	0.8552	0.8781	0.9372	0.0613
Lung lobes 2 (CD31)	0.6032	0.7484	0.8239	0.0243
Lung lobes 3 (CD31)	0.5815	0.7324	0.7853	0.0303
Mice kidney 2 (CD31)	0.5492	0.7779	0.8765	0.0626
Lung lobes 4 (HE)	0.5490	0.8059	0.8582	0.0925
Lung lobes 5 (CD31)	0.5481	0.7383	0.7779	0.0533
Myoma (H&E)	0.9011	0.8961	0.9305	0.0218

Figures 9 and 10 below contain example tissue pairs from ANHIR and myoma datasets. Source and target images are used as an input and the common information is extracted in the computational transformations. The proposed method detects the keypoints on images and then examines the feature matching. After detecting and matching the keypoints, the features are selected and combined to create the registered image.

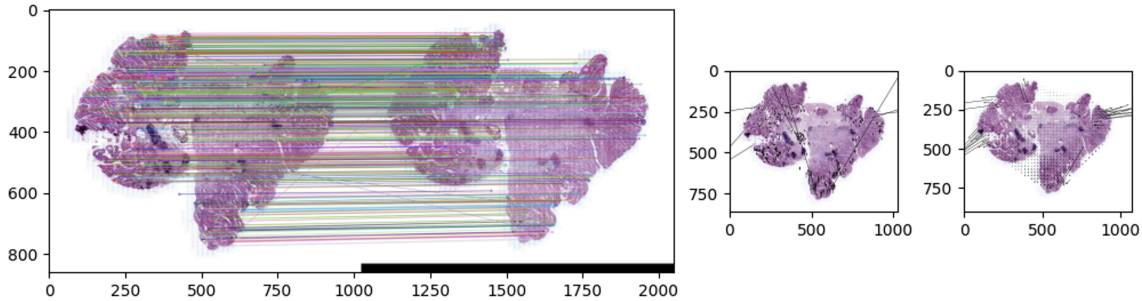

Figure 9. Feature matching and registration results on an example image pair of ANHIR dataset.

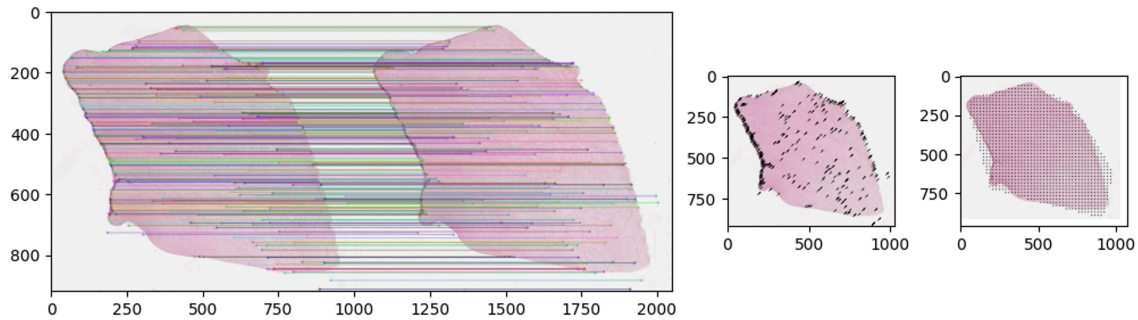

Figure 10. Feature matching and registration results on an example image pair of myoma dataset.

Figures 11 and 12 represent registered whole slide images with visualized target registration error lines. Two images, source and registered ones, are on top of each other creating one image with landmarks and borderlines from both images. TRE is used to calculate the registration error of those differences between the landmarks. Green dots visualize the original position of landmarks, red dots visualize the target positions, and blue dots stand for estimate positions. The red lines visualize TRE.

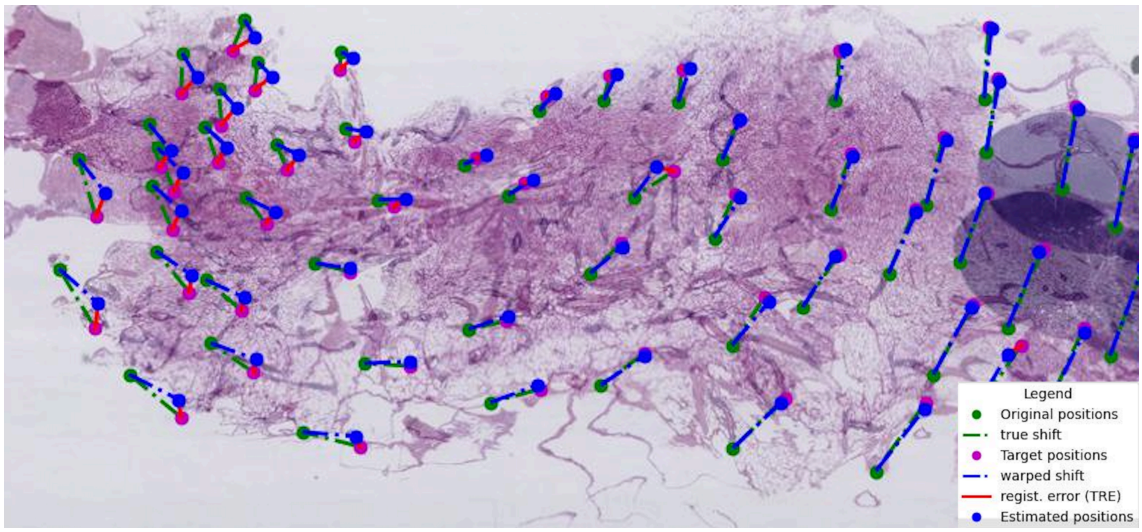

Figure 11. Part of mammary gland WSI with visualized target registration error. Source and registered images on top of each other with aligned landmarks.

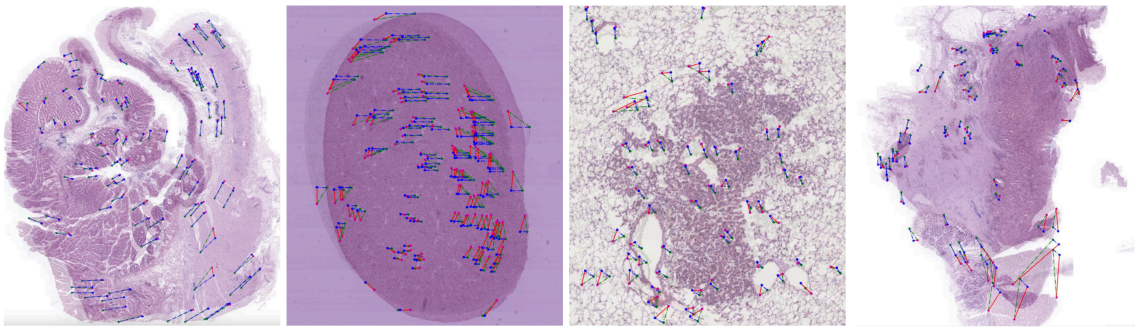

Figure 12. Visualized target registration error on COAD, mice kidney, lung lesion, and other COAD tissues.

Different registration algorithms were compared with the proposed method and their average rTRE, median rTRE, and max rTRE values were calculated. Also, algorithm's robustness was observed and it is shown for each method. The state-of-the-art methods are represented first, and the proposed method is shown in the last row. The results vary depending on the used algorithm while each method has its own strength. The results for the evaluation set are presented exclusively in table 5. Figure 13 visualizes the average rTRE, median rTRE, Max rTRE values and robustness of the reference methods on the test dataset.

Table 5. Quantitative results of state-of-the-art methods comparing with proposed method. The results for the evaluation set are presented exclusively.

Method	**Average rTRE**		**Median rTRE**		**Max rTRE**		**Robustness**	
	Average	**Median**	**Average**	**Median**	**Average**	**Median**	**Average**	**Median**
AGH	0.0073	0.0032	0.0036	0.0017	0.0290	0.0214	0.9795	1.0000
UPENN	0.0041	0.0029	0.0029	0.0019	0.0238	0.0190	0.9898	1.0000
CKVST	0.0042	0.0027	0.0026	0.0023	0.0239	0.0189	0.9883	1.0000
TUB	0.0089	0.0029	0.0077	0.0021	0.0280	0.0178	0.9845	1.0000
TUNI	0.0063	0.0031	0.0048	0.0021	0.0287	0.0204	0.9822	1.0000
MEVIS	0.0043	0.0028	0.0028	0.0018	0.0251	0.0188	0.9880	1.0000
UA	0.0536	0.0100	0.0506	0.0082	0.1124	0.0353	0.8209	0.9852
bUnwarpJ	0.1097	0.0290	0.1105	0.0260	0.1995	0.0727	0.7899	0.9310
NiftyReg	0.1120	0.0372	0.1136	0.0355	0.2010	0.0714	0.7427	0.8519
Elastix	0.0964	0.0074	0.0956	0.0054	0.1857	0.0353	0.8477	0.9722
DeepHistReg	0.0061	0.0033	0.0047	0.0019	0.0276	0.0224	0.9799	1.0000
Proposed Method	0.0059	0.0030	0.0043	0.0015	0.0272	0.0221	0.9825	1.0000

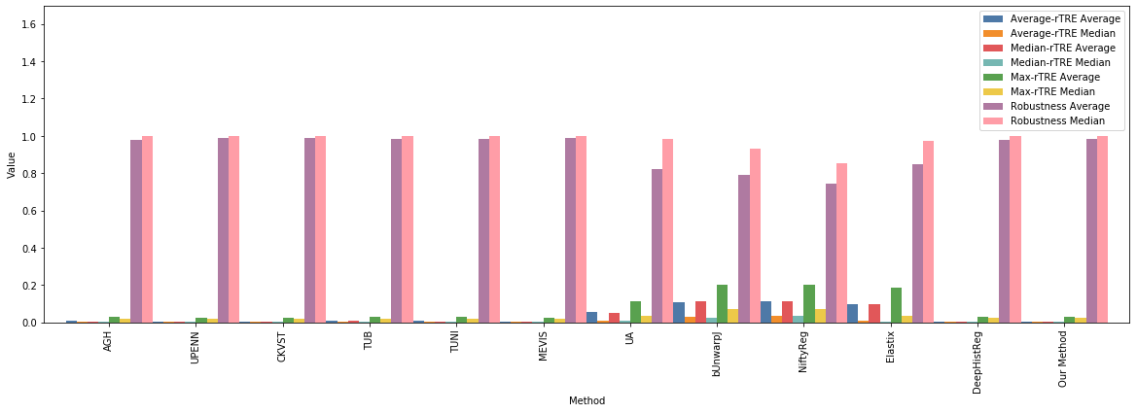

Figure 13. Average rank of average rTRE, median rTRE, Max rTRE and robustness per reference method on the test dataset.

Beside the good results of rTRE values of our proposed method, the registered image may sometimes have a massive rTRE value that does not fit in the range of acceptable values. It can be caused by the unfocused parts of the scanned tissues, big dataset with many kinds of tissues and heterogenic images, used algorithm, differences in sifts, and scaling and orientation between the source and reference images. Some other nonideal features can also occur and cause the bad results. The color of stained tissue image may be very light and unnoticeable, and even unsuccessful in some cases. Also, some artifacts were observed during this work and they may cause incorrect focus area when processing the images.

6 DISCUSSION

Based on the results of this work, the registration steps including stain color feature augmentation and keypoints matching lead to the expected results. The modifications used in proposed method can provide more opportunities to register images in .mha format instead of gray scaling. Several steps are used to process the whole slide image from background segmentation to non-rigid registration. As the ANHIR dataset is public and available with its 50+ histological sets and 8 different types of tissues, it is important to perform the tests with each tissue set to get reliable and comparable results. Every ANHIR image set contains WSIs, each corresponding to a tissue cut from the same sample and dyed with a different stain [39]. In this thesis work only part of the ANHIR image sets was used. Observed WSIs were taken from each tissue type to allow the results being analyzed and reproducible. Myoma dataset was used as well. Using multiple image sets clarifies the capabilities and limitations of the tested methods.

During this study many new ideas were born and some of them may see the daylight in the near future. Probably panoramic view could be utilized more often during the process of registration. In addition, optimization of testing and preprocessing parts might give an advantage when registering different kinds of images with properties specific to them. However, those ideas were not covered in this time of period due to the main focus being on stain color feature augmentation of image registration technique development. Also, the topic of image registration techniques in digital pathology being wide, some limitations had to be set to the scope of this work.

It is predicted that DL allows recently developed computational staining techniques, probably better known as virtual staining, being applied on unstained slide tissue sections using modalities such as autofluorescence, quantitative phase imaging, or hyperspectral imaging. Virtual staining of these so-called label-free tissues not only reduce the high costs and faster staining, but it also allows the examiner to perform advanced analysis on the tissue [35]. Some previous studies have given a little taste of protocols that combine classical histological methods with modern 3D image filtering and visualization techniques. Then small but complex biological specimens could be visualized in high-resolution 3D illustrations by the serial sections of virtual reality. Also, an idea of 3D models embedded in digital publications like PDFs is reported. Embedded polygon-surfaces could give a great extra value for PDFs and other digital articles [34, 90]. In the area of whole slide image registration, creating more robust algorithm handling full resolution WSIs is recommended as it would be helpful to be able to avoid the current registration challenges [30]. Faster computational time and memory saving methods would be ideal improvements.

7 CONCLUSIONS

Our world is changing rapidly, and technology and new innovative ideas are taking more and more place. Medical applications, such as scanning and analyzing diseases via images, also should be upgraded to this day, and digitalizing pathology has been a huge step into it. Digital pathology opens doors for universal imaging and processing technologies, everywhere at the same time. Whole slide images enable pathologists and other experts to work with the patient wherever they are. There are still new challenges waiting for the further studies and it will be an interesting journey to see how its capacity is going to be used in the future.

Being challenging task to observe and analyze the whole slide images, landmark validation is a potential tool to find the similarities and special information from the virtualized tissue images. Usually, the H&E stain is used as it dyes the tissue in purple and pinkish shade and is then easier to obtain by a human eye. To work on a tissue of interest, in most of the cases it needs to be processed somehow after scanning and digitalizing. Contrast the colors by stain augmentation helps to separate the structures of the sample. Sometimes also color normalization is used to get more robustness.

As in traditional pathology, the tissue of interest is observed at microscopic level but instead of manual microscopy the computer screen is used. Normally, the tissue sample is first cut from the patient and then prepared as clearing, sectioning, and staining before scanning into virtual tissue slide. During preprocessing the image pairs go through padding and parsing from common image formats into uncompressed forms to speeding up the image loading phase. Size of one whole slide image can be few gigabytes (the SVS images studied in this work had usually the size from 2 to 5 GB) and that is why downsampling is mostly used in preprocessing phases. Downsampling can decrease the processing and registration time notably and hence make the process more efficient and less time consuming. Also, background segmentation, initial alignment, and affine registration are utilized before non-rigid registration.

Big step has been taken when deep learning and artificial intelligence found their place in medical technology. With their help the processes can be automatized while the state-of-the-art algorithms work for us. There are several registration methods being measured the algorithms' quality, including the proposed method of this study but also the algorithms known as DeepHistReg, Elastix, and bUnwarpJ for instance. Development of digital pathology imaging is universally common mission and back in the days the ANHIR challenge was open to everyone sharing the public dataset and results of former competitions.

In this work the most significant evaluation metrics were PCC, SSIM, FSIM, RMSE, rTRE and robustness when myoma and ANHIR datasets were studied and processed. Regarding to the results, our method performs very well and the output of the registration meets our expectations. This study area contains many interesting topics to cover for

future work. Challenges of this work were limited amount of time, some development and testing parts of the proposed method, and various types of tissues on small size of the datasets we used. One suggestion for the further studies is to focus on how to manage many sorts of data and details on larger dataset. Testing and processing different kinds of tissue images can diversify the registration systems and provide more reliable results in the future. Also, the evaluation metrics could be observed, depending on the current validation and application.

8 REFERENCES

[1] Kurc T, Bakas S, Ren X, Bagari A, Momeni A, Huang Y, Zhang L, Kumar A, Thibault M, Qi Q, Wang Q. (2020) Segmentation and classification in digital pathology for glioma research: challenges and deep learning approaches. Frontiers in Neuroscience, 14. DOI: https://doi.org/10.3389/fnins.2020.00027.

[2] Azevedo Tosta TA, de Faria PR, Neves LA, do Nascimento MZ. (2019) Computational normalization of H&E-stained histological images: Progress, challenges and future potential. Artificial Intelligence in Medicine, 95: 118-132. DOI: https://doi.org/10.1016/j.artmed.2018.10.004.

[3] Hoque MZ, Keskinarkaus A, Nyberg P, Seppänen T. (2021) Retinex model based stain normalization technique for whole slide image analysis. Computerized Medical Imaging and Graphics, 90: 101901. DOI: https://doi.org/10.1016/j.compmedimag.2021.101901.

[4] Niazi MKK, Parwani AV, Gurcan MN. (2019) Digital pathology and artificial intelligence. The Lancet Oncology, 20(5): 253-261. DOI: https://doi.org/10.1016/S1470-2045(19)30154-8.

[5] Zheng Y, Jiang Z, Zhang H, Xie F, Shi J, Xue C. (2019) Adaptive color deconvolution for histological WSI normalization. Computer Methods and Programs in Biomedicine, 170: 107-120. DOI: https://doi.org/10.1016/j.cmpb.2019.01.008.

[6] Ciompi F, Geessink O, Bejnordi BE, de Souza GS, Baidoshvili A, Litjens G, van Ginneken B, Nagtegaal I, van der Laak J. (2017) The importance of stain normalization in colorectal tissue classification with convolutional networks. IEEE 14th International Symposium on Biomedical Imaging (ISBI 2017): 160-163. DOI: https://doi.org/10.1109/ISBI.2017.7950492.

[7] Barisoni L, KJ. Lafata, Hewitt SM, Madabhushi A, Balis UGJ. (2020) Digital pathology and computational image analysis in nephropathology. Nature Reviews Nephrology, 16: 669-685. DOI: https://doi.org/10.1038/s41581-020-0321-6.

[8] Roy S, kumar Jain A, Lal S, Kini J. (2018) A study about color normalization methods for histopathology images. Micron, 114: 42-61. DOI: https://doi.org/10.1016/j.micron.2018.07.005.

[9] Janowczyk A, Madabhushi A. (2016) Deep learning for digital pathology image analysis: A comprehensive tutorial with selected use cases. Journal of Pathology Informatics, 7(1): 29. DOI: https://doi.org/10.4103/2153-3539.186902.

[10] Aeffner F, Zarella MD, Buchbinder N, Bui MM, Goodman MR, Hartman DJ, Lujan GM, Molani MA, Parwani AV, Lillard K, Turner OC, Vemuri VNP, Yuil-Valdes AG, Bowman D. (2018) Introduction to Digital Image Analysis in Whole-slide Imaging: A White Paper from the Digital Pathology Association. Journal of Pathology Informatics, 10(1): 9. DOI: https://doi.org/10.4103/jpi.jpi_82_18.

[11] Griffin J, Treanor D. (2017) Digital pathology in clinical use: where are we now and what is holding us back? Histopathology, 70(1): 134-145. DOI: https://doi.org/10.1111/his.12993.

[12] Madabhushi A. (2009) Digital pathology image analysis: opportunities and challenges. Imaging Med, 1(1): 7-10. URL: https://pubmed.ncbi.nlm.nih.gov/30147749/.

[13] Snead DRJ, Tsang Y-W, Meskiri A, Kimani P K, Crossman R, Rajpoot NM, Blessing E, Chen K, Gopalakrishnan K, Matthews P, Momtahan N, Read-Jones S, Sah S, Simmons E, Sinha B, Suortamo S, Yeo Y, El Daly H, Cree IA. (2015) Validation of digital pathology imaging for primary histopathological diagnosis. Histopathology, 68(7): 1063-1072. DOI: https://doi.org/10.1111/his.12879.

[14] Borovec J, Munoz-Barrutia A, Kybic J. (2018) Benchmarking of Image Registration Methods for Differently Stained Histological Slides. 25th IEEE International Conference on Image Processing (ICIP): 3368-3372. DOI: https://doi.org/10.1109/ICIP.2018.8451040.

[15] Wyawahare MV, Patil PM, Abhyankar HK. (2009) Image Registration Techniques: An overview. International Journal of Signal Processing, Image Processing and Pattern Recognition, 2 (3).

[16] Crum WR, Hartkens T, Hill DLG. (2004) Non-rigid image registration: theory and practice. The British Journal of Radiology, 77(2): 107-208. DOI: https://doi.org/10.1259/bjr/25329214.

[17] Brock KK, Mutic S, McNutt TR, Li H, Kessler ML. (2017) Use of image registration and fusion algorithms and techniques in radiotherapy: Report of the AAPM Radiation Therapy Committee Task Group No. 132. Medical Physics, 44(7): 43-76. DOI: https://doi.org/10.1002/mp.12256.

[18] Van Essen DC, Smith SM, Barch DM, Behrens TE, Yacoub E, Ugurbil K. (2013) WU-Minn HCP Consortium, the WU-Minn human connectome project: an overview. NeuroImage, 80: 62-79. DOI: https://doi.org/10.1016/j.neuroimage.2013.05.041.

[19] Yang X, Kwitt R, Styner M, Niethammer M. (2017) Quicksilver: Fast predictive image registration - A deep learning approach. NeuroImage, 158: 378-396. DOI: https://doi.org/10.1016/j.neuroimage.2017.07.008.

[20] Zhang C, Jiang Y, Li N, Zhang Z, Islam MT, Dai J, Liu L, He W, Qin W, Xiong J, Xie Y, Liang X. (2022) A Hybrid Deep Feature-Based Deformable Image Registration Method for Pathological Images. DOI: https://doi.org/10.48550/arXiv.2208.07655.

[21] Wang S, Yang DM, Rong R, Zhan X, Fujimoto J, Liu H, Minna J, Wistuba II, Xie Y, Xiao G. (2019) Artificial Intelligence in Lung Cancer Pathology Image Analysis. Cancers, 11 (11): 1673; DOI: https://doi.org/10.3390/cancers11111673.

[22] Al-Janabi S, Huisman A, van Diest PJ. (2012) Review: Digital pathology: current status and future perspectives. Histopathology, 61: 1-9. DOI: https://doi.org/10.1111/j.1365-2559.2011.03814.x.

[23] Hanna MG, Parwani A, Sirintrapun SJ. (2020) Whole Slide Imaging: Technology and Applications. Advances In Anatomic Pathology, 27(4): 251-259. DOI: https://doi.org/10.1097/PAP.0000000000000273.

[24] Tschuchnig ME, Oostingh GJ, and Michael Gadermayr M. (2020) Generative Adversarial Networks in Digital Pathology: A Survey on Trends and Future Potential. Patterns, 1(6): 100089. DOI: https://doi.org/10.1016/j.patter.2020.100089.

[25] Farahani N, Parwani AV, Pantanowitz L. (2015) Whole slide imaging in pathology: advantages, limitations, and emerging perspectives. Pathology and Laboratory Medicine International, 7: 23-33. DOI: http://dx.doi.org/10.2147/PLMI.S59826.

[26] Meijer GA, Beliën JAM, van Diest PJ, Baak JPA. (1997) Image analysis in clinical pathology. Journal of Clinical Pathology, 50(5): 365-370. DOI: https://doi.org/10.1136/jcp.50.5.365.

[27] Borovec J, Kybic J, Arganda-Carreras I, Sorokin DV, Bueno G, Khvostikov AV, Bakas S, Chang EI-C, Heldmann S, Kartasalo K, Latonen L, Lotz J, Noga M, Pati S, Punithakumar K, Ruusuvuori P, Skalski A, Tahmasebi N, Valkonen M, Venet L, Wang Y, Weiss N, Wodzinski M, Xiang Y, Xu Y, Yan Y, Yushkevich P, Zhao S,

Muñoz-Barrutia A. (2020) ANHIR: Automatic Non-rigid Histological Image Registration Challenge, IEEE Transactions on Medical Imaging, 39(10): 3042-3052. DOI: https://doi.org/10.1109/TMI.2020.2986331.

[28] Wodzinski M, Müller H. (2020) DeepHistReg: Unsupervised Deep Learning Registration Framework for Differently Stained Histology Samples. Computer Methods and Programs in Biomedicine, 198: 105799. DOI: https://doi.org/10.1016/j.cmpb.2020.105799.

[29] Gurcan MN, Boucheron L, Can A, Madabhushi A, Rajpoot N, Yener B. (2009) Histopathological image analysis: a review. IEEE Reviews in Biomedical Engineering, 2: 147-171. DOI: https://doi.org/10.1109/RBME.2009.2034865.

[30] Hoque MZ, Keskinarkaus A, Nyberg P, Mattila T, Seppänen T. (2022) Whole slide image registration via multi-stained feature matching. Computers in Biology and Medicine, 144: 105301. DOI: https://doi.org/10.1016/j.compbiomed.2022.105301.

[31] Lopez XM, D'Andrea E, Barbot P, Bridoux A-S, Rorive S, Salmon I, Debeir O, Decaestecker C. (2013) An automated blur detection method for histological whole slide imaging. PLoS ONE, 8(12): e82710. DOI: https://doi.org/10.1371/journal.pone.0082710.

[32] Alsubaie N, Trahearn N, Raza SEA, Snead D, Rajpoot NM. (2017) Stain Deconvolution Using Statistical Analysis of Multi-Resolution Stain Colour Representation. PLoS ONE, 12(1): e0169875. DOI: https://doi.org/10.1371/journal.pone.0169875.

[33] Kofler L, Breuninger H, Schreiber RH, Eichner M, Häfner M-H, Schnabl SM. (2021) Three-dimensional histology vs. serial section histology in the treatment of primary basal cell carcinoma: arandomized, prospective, blinded study of 569 tumours. JEADV, 35(6): 1323-1330. DOI: https://doi.org/10.1111/jdv.17155.

[34] Handschuh S, Schwaha T, Metscher BD. (2010) Showing their true colors: a practical approach to volume rendering from serial sections. BMC Developmental Biology, 10(41). URL: http://www.biomedcentral.com/1471-213X/10/41.

[35] de Haan K, Zhang Y, Zuckerman JE, Liu T, Sisk AE, Diaz MFP, Jen K-Y, Nobori A, Liou S, Zhang S, Riahi R, Rivenson Y, Wallace WD, Ozcan A. (2021) Deep learning-based transformation of H&E stained tissues into special stains. Nature Communications, 12(4884). DOI: https://doi.org/10.1038/s41467-021-25221-2.

[36] Tellez D, Litjens G, Bándi P, Bulten W, Bokhorst J-M, Ciompi F, van der Laak J. (2019) Quantifying the effects of data augmentation and stain color normalization

in convolutional neural networks for computational pathology. Medical Image Analysis, 58: 101544. DOI: https://doi.org/10.1016/j.media.2019.101544.

[37] Lotz J, Weiss N, van der Laak J, Heldmann S. (2022) Comparison of Consecutive and Re-stained Sections for Image Registration in Histopathology. DOI: https://doi.org/10.48550/arXiv.2106.13150.

[38] Wodzinski M, Skalski A. (2021) Multistep, automatic and non-rigid image registration method for histology samples acquired using multiple stains. Physics in Medicine & Biology, 66: 025006. DOI: https://doi.org/10.1088/1361-6560/abcad7.

[39] Grand Challenge. Challenges, ANHIR, Dataset. URL: https://anhir.grand-challenge.org/Data/. Accessed 24.03.2023.

[40] El-Baz A, Yuksel SE, Elshazly S, Farag AA. (2005) Non-rigid registration techniques for automatic follow-up of lung nodules. International Congress Series, 1281: 1115-1120. DOI: https://doi.org/10.1016/j.ics.2005.03.340.

[41] Pauly M, Mitra NJ, Giesen J, Gross MH, Guibas LJ. (2005) Example-Based 3D Scan Completion. Eurographics Symposium on Geometry Processing: 23-32.

[42] Almazán J, Fornés A, Valveny E. (2012) A non-rigid appearance model for shape description and recognition. Pattern Recognition, 45(9): 3105-3113. DOI: https://doi.org/10.1016/j.patcog.2012.01.010.

[43] Efros AA, Freeman WT. (2001), Image quilting for texture synthesis and transfer. Association for Computing Machinery, 28th annual conference on Computer graphics and interactive techniques: 341-346. DOI: https://doi.org/10.1145/383259.383296.

[44] Schulman J, Ho J, Lee C, Abbeel P. (2016) Learning from Demonstrations Through the Use of Non-Rigid Registration. Robotics Research. Springer Tracts in Advanced Robotics, 114: 339-354. DOI: https://doi.org/10.1007/978-3-319-28872-7_20.

[45] Rigaud B, Simon A, Castelli J, Lafond C, Acosta O, Haigron P, Cazoulat G, de Crevoisier R. (2019) Deformable image registration for radiation therapy: principle, methods, applications and evaluation. Acta Oncologica, 58(9): 1225-1237. DOI: https://doi.org/10.1080/0284186X.2019.1620331.

[46] Chen CW, Huang TS, Arrott M. (1994) Modeling, analysis and visualization of left ventricle shape and motion by hierarchical decomposition. IEEE Transactions on

Pattern Analysis and Machine Intelligence, 16(4): 342-356. DOI: https://doi.org/10.1109/34.277589.

[47] Tellez D, Balkenhol M, Karssemeijer N, Litjens G, van der Laak J, Ciompi F. (2018) H&E stain augmentation improves generalization of convolutional networks for histopathological mitosis detection. Medical Imaging 2018: Digital Pathology, 10581(105810Z). DOI: https://doi.org/10.1117/12.2293048.

[48] Wang J, MacKenzie JD, Ramachandran R, Chen DZ. (2014) Identifying Neutrophils in H&E Staining Histology Tissue Images. Medical Image Computing and Computer-Assisted Intervention. MICCAI 2014. Lecture Notes in Computer Science, 8673: 73-80. DOI: https://doi.org/10.1007/978-3-319-10404-1_10.

[49] Nguyen L, Tosun AB, Fine JL, Lee AV, Taylor DL, Chennubhotla SC. (2018) Spatial statistics for segmenting histological structures in H&E stained tissue images. IEEE Transactions on Medical Imaging, 36(7): 1522-1532. DOI: https://doi.org/10.1109/TMI.2017.2681519.

[50] McCann MT. (2015). Tools for Automated Histology Image Analysis. Carnegie Mellon University, Thesis: 5-12. DOI: https://doi.org/10.1184/R1/6723926.v1.

[51] Rivenson Y, Wang H, Wei Z, de Haan K, Zhang Y, Wu Y, Günaydın H, Zuckerman JE, Chong T, Sisk AE, Westbrook LM, Wallace WD, Ozcan A. (2019) Virtual histological staining of unlabelled tissue-autofluorescence images via deep learning. Nature Biomedical Engineering, 3: 466-477. DOI: https://doi.org/10.1038/s41551-019-0362-y.

[52] Gupta A, Duggal R, Gehlot S, Gupta R, Mangal A, Kumar L, Thakkar N, Satpathy D. (2020) Geometry-inspired chemical and tissue invariant stain normalization of microscopic medical images. Medical Image Analysis, 65: 101788. DOI: https://doi.org/10.1016/j.media.2020.101788.

[53] Noothout JMH, de Vos BD, Wolterink JM, Postma EM, Smeets PAM, Takx RAP, Leiner T, Viergever MA, Išgum I. (2020) Deep Learning-Based Regression and Classification for Automatic Landmark Localization in Medical Images. IEEE Transactions on Medical Imaging, 39(12): 4011-4022. DOI: https://doi.org/10.1109/TMI.2020.3009002.

[54] Xiao Y, Decencière E, Velasco-Forero S, Burdin H, Bornschlögl T, Bernerd F, Warrick E, Baldeweck T. (2019) A new color augmentation method for deep learning segmentation of histological images. IEEE 16th International Symposium on Biomedical Imaging: 886-890. DOI: https://doi.org/10.1109/ISBI.2019.8759591.

[55] Arévalo J, Cruz-Roa A, González FA. (2014) Histopathology image representation for automatic analysis: a state of the art review. Revista Med, 22(2): 79-91.

[56] Akbari H, Halig LV, Zhang HZ, Wang DS, Chen ZG, Fei BW. (2012) Detection of Cancer Metastasis Using a Novel Macroscopic Hyperspectral Method. Medical Imaging 2012: Biomedical Applications in Molecular, Structural, and Functional Imaging, 8673: 831711. DOI: https://doi.org/10.1117/12.912026.

[57] Glocker B, Sotiras A, Komodakis N, Paragios N. (2011) Deformable Medical Image Registration: Setting the State of the Art with Discrete Methods. Annual Review of Biomedical Engineering, 13: 219-244. DOI: https://doi.org/10.1146/annurev-bioeng-071910-124649.

[58] Kooi T, Litjens G, van Ginneken B, Gubern-Mérida A, Sánchez CI, Mann R, den Heeten A, Karssemeijer N. (2017). Large scale deep learning for computer aided detection of mammographic lesions. Medical Image Analysis, 35: 303-312. DOI: https://doi.org/10.1016/j.media.2016.07.007.

[59] Simonyan K, Zisserman A. (2015) Very Deep Convolutional Networks for Large-Scale Image Recognition. Published as a conference paper at ICLR 2015. DOI: https://doi.org/10.48550/arXiv.1409.1556.

[60] Zhao S, Lau T, Luo J, Chang E, Xu Y. (2019) Unsupervised 3D End-to-End Medical Image Registration with Volume Tweening Network. IEEE Journal of Biomedical and Health Informatics, 24(5): 1394-1404. DOI: https://doi.org/10.1109/JBHI.2019.2951024.

[61] Salehi M, Sadr AV, Mahdavi SR, Arabi H, Shiri I, Reiazi R. (2022) Deep Learning-based Non-rigid Image Registration for High-dose Rate Brachytherapy in Inter-fraction Cervical Cancer. Journal of Digital Imaging, 36: 574-587. DOI: https://doi.org/10.1007/s10278-022-00732-6.

[62] McQuin C, Goodman A, Chernyshev V, Kamentsky L, Cimini BA, Karhohs KW, Doan M, Ding L, Rafelski SM, Thirstrup D, Wiegraebe W, Singh S, Becker T, Caicedo JC, Carpenter AE. (2018) CellProfiler 3.0: Next-generation image processing for biology. PLOS Biology, 16(7): e2005970. DOI: https://doi.org/10.1371/journal.pbio.2005970.

[63] Maier A, Syben C, Lasser T, Riess C. (2018) A gentle introduction to deep learning in medical image processing. Zeitschrift für Medizinische Physik, 29(2): 86-101. DOI: https://doi.org/10.1016/j.zemedi.2018.12.003.

[64] Hellier P, Barillot C, Corouge I, Gibaud B, Le Goualher G, Collins DL, Evans A, Malandain G, Ayache N, Christensen GE, Johnson HJ. (2003) Retrospective evaluation of intersubject brain registration. IEEE Transactions on Medical Imaging, 22(9): 1120-1130. DOI: https://doi.org/10.1109/TMI.2003.816961.

[65] Lowe DG. (2004) Distinctive image features from scale-invariant keypoints. International Journal of Computer Vision, 60: 91-110. DOI: https://doi.org/10.1023/B:VISI.0000029664.99615.94.

[66] Rublee E, Rabaud V, Konolige K, Bradski G. (2011) ORB: an efficient alternative to SIFT or SURF. International Conference on Computer Vision, IEEE, 2011: 2564-2571. DOI: https://doi.org/10.1109/ICCV.2011.6126544.

[67] Bay H, Ess A, Tuytelaars, van Gool L. (2018) Speeded-Up Robust Features (SURF). Computer Vision and Image Understanding, 110(3): 346-359. DOI: https://doi.org/10.1016/j.cviu.2007.09.014.

[68] Zitová B. (2018) Mathematical Approaches for Medical Image Registration. Reference Module in Biomedical Sciences, 2019: 21-32. DOI: https://doi.org/10.1016/B978-0-12-801238-3.99990-2.

[69] Klein A, Andersson J, Ardekani BA, Ashburner J, Avants B, Chiang M-C, Christensen GE, Collins DL, Gee J, Hellier P, Song JH, Jenkinson M, Lepage C, Rueckert D, Thompson P, Vercauteren T, Woods RP, Mann JJ, Parsey RV. (2009) Evaluation of 14 nonlinear deformation algorithms applied to human brain MRI registration. NeuroImage, 46(3): 786-802. DOI: https://doi.org/10.1016/j.neuroimage.2008.12.037.

[70] Sotiras A, Davatzikos C. (2013) Deformable Medical Image Registration: A Survey. IEEE Transactions on Medical Imaging, 32(7): 1153-1190. DOI: https://doi.org/10.1109/TMI.2013.2265603.

[71] Oliveira FPM, Tavares JMRS. (2012) Medical image registration: a review. Computer Methods in Biomechanics and Biomedical Engineering 2014, 17(2): 73-93. DOI: https://doi.org/10.1080/10255842.2012.670855.

[72] Klein S, Staring M, Murphy K, Viergever MA, Pluim JPW. (2010) Elastix: A Toolbox for Intensity-Based Medical Image Registration. IEEE Transactions on Medical Imaging, 29(1): 196-205. DOI: https://doi.org/10.1109/TMI.2009.2035616.

[73] Modat M, Cash DM, Daga P, Winston GP, Duncan JS, Ourselin S. (2014) A symmetric block-matching framework for global registration. Proc. SPIE, 9034(90341D). DOI: https://doi.org/10.1117/12.2043652.

[74] Rueckert D, Sonoda LI, Hayes C, Hill DLG, Leach MO, Hawkes DJ. (1999) Nonrigid registration using free-form deformations: application to breast MR images. IEEE Transactions on Medical Imaging, 18(8): 712-721. DOI: https://doi.org/10.1109/42.796284.

[75] Arganda-Carreras I, Sorzano COS, Marabini R, Carazo JM, Ortiz-de-Solorzano C, Kybic J. (2006). Consistent and Elastic Registration of Histological Sections Using Vector-Spline Regularization. Computer Vision Approaches to Medical Image Analysis. CVAMIA 2006. Lecture Notes in Computer Science, 4241: 85-95. DOI: https://doi.org/10.1007/11889762_8.

[76] Brown LG. (1992) Survey of Image Registration Techniques. ACM Computing Surveys, 24(4): 325-376. DOI: https://doi.org/10.1145/146370.146374.

[77] Lotz J, Olesch J, Müller B, Polzin T, Galuschka P, Lotz JM, Heldmann S, Laue H, González-Vallinas, Warth A, Lahrmann B, Grabe N, Sedlaczek O, Breuhahn K, Modersitzki J. (2016) Patch-based nonlinear image registration for gigapixel whole slide images. IEEE Transactions on Biomedical Engineering, 63(9): 1812-1819. DOI: https://doi.org/10.1109/TBME.2015.2503122.

[78] Alcantarilla PF, Bartoli A, Davison AJ. (2012) KAZE features. Computer Vision. ECCV 2012: 214-227. DOI: https://doi.org/10.1007/978-3-642-33783-3_16.

[79] Veena Divya K, Jatti A, Joshi R, Deepu Krishna S. (2022) Characterization of Dental Pathologies using Digital Panoramic X-Ray Images based on Texture Analysis. 39th Annual International Conference of the IEEE Engineering in Medicine and Biology Society: 592-595, DOI: https://doi.org/10.1109/EMBC.2017.8036894.

[80] Szeliski R, Shum H-Y. (1997) Creating Full View Panoramic Image Mosaics and Environment Maps. Microsoft Research.

[81] Zitová B, Flusser J. (2003) Image Registration Methods: A Survey. Image and Vision Computing, 21(11): 977-1000. DOI: https://doi.org/10.1016/S0262-8856(03)00137-9.

[82] Nurmenniemi S, Sinikumpu T, Alahuhta I, Salo S, Sutinen M, Santala M, Risteli J, Nyberg P, Salo T. (2009) A novel organotypic model mimics the tumor

microenvironment. The American journal of pathology, 175(3): 1281-1291. DOI: https://doi.org/10.2353/ajpath.2009.081110.

[83] Chang J-R, Wu M-S, Yu W-H, Chen C-C, Yang C-K, Lin Y-Y, Yeh C-Y. (2021) Stain Mix-Up: Unsupervised Domain Generalization for Histopathology Images. Medical Image Computing and Computer Assisted Intervention. MICCAI 2021. Lecture Notes in Computer Science, 12903: 117-126. DOI: https://doi.org/10.1007/978-3-030-87199-4_11.

[84] Beer A, Beer P. (1852) Determination of the absorption of red light in colored liquids. Annalen der Physik und Chemie 86(5): 78-88.

[85] Ronneberger O, Fischer P, Brox T. (2015) U-Net: Convolutional Networks for Biomedical Image Segmentation. Medical Image Computing and Computer-Assisted Intervention. MICCAI 2015. Lecture Notes in Computer Science, 9351: 234-241. DOI: https://doi.org/10.1007/978-3-319-24574-4_28.

[86] He K, Zhang X, Ren S, Sun J. (2016) Deep Residual Learning for Image Recognition. Proceedings of the IEEE Conference on Computer Vision and Pattern Recognition, 2016: 770-778. URL: https://openaccess.thecvf.com/content_cvpr_2016/papers/He_Deep_Residual_Learning_CVPR_2016_paper.pdf. Accessed 16.06.2023.

[87] Dive Into Deep Learning. Chapter 7.6. Residual Networks (ResNet). URL: https://classic.d2l.ai/chapter_convolutional-modern/resnet.html. Accessed 16.06.2023.

[88] Microscopes International. (04.08.2022) Question: What are Tiled TIFF (SVS) Files? URL: https://www.microscopesinternational.com/support/kb/article/ngn1266.aspx. Accessed 25.03.2023.

[89] Cohen EAK, D. Ober K, Ober RJ. (2015) Cramér-Rao Lower Bound for Point Based Image Registration With Heteroscedastic Error Model for Application in Single Molecule Microscopy. IEEE Transactions on Medical Imaging, 34(12): 2632-2644. DOI: https://doi.org/10.1109/TMI.2015.2451513.

[90] Ruthensteiner B, Heß M. (2008) Embedding 3D Models of Biological Specimens in PDF Publications. Microscopy Research & Technique, 71(11): 778-786 7. DOI: https://doi.org/10.1002/jemt.20618.